AN ANALYTICAL FINITE ELEMENT TECHNIQUE FOR PREDICTING THRUST FORCE AND TORQUE IN DRILLING PROCESS

A thesis submitted in partial fulfillment of the requirement for the award of degree of

MASTER OF ENGINEERING
IN
CAD/CAM & ROBOTICS

Submitted By

ASHISH MITTAL
(800881003)

Under the Guidance of

Mr. J. S. SAINI
Asst. Professor, Mechanical Engg. Deptt.
Thapar University, Patiala

MECHANICAL ENGINEERING DEPARTMENT
THAPAR UNIVERSITY, PATIALA-147004
JULY, 2010

CERTIFICATE

I hereby declare that the work which is being presented in this thesis entitled, **"AN ANALYTICAL FINITE ELEMENT TECHNIQUE FOR PREDICTING THRUST FORCE AND TORQUE IN DRILLING PROCESS"** in partial fulfillment of requirement for the award of the **MASTER OF ENGINEERING IN CAD/CAM & ROBOTICS** submitted in the **MECHANICAL ENGINEERING DEPARTMENT OF THAPAR UNIVERSITY, PATIALA,** is an authentic record of the initial work carried out by me under the guidance of **Mr. J. S. SAINI, Asst. Professor, Mechanical Engineering Department, Thapar University, Patiala** and refers other researcher's works which is dully listed in the references section.

The matter embodied in this thesis has not been submitted in part or full to any other university or institute for the award of any degree.

Dated: 15 July '10

Ashish Mittal

(ASHISH MITTAL)

This is to certify that above declaration made by the student concerned is correct to the best of my knowledge & belief.

(Mr. J. S. SAINI) 16/7/10

Asst. Professor, MED

Thapar University, Patiala

Countersigned by

(Dr. S. K. MOHAPATRA)

Professor & Head, MED

Thapar University, Patiala

R K Sharma 29.7.10

(Dr. R. K. SHARMA)

Dean, Academic Affairs

Thapar University, Patiala

ACKNOWLEDGEMENT

Words are often less to revels one's deep regards. With an understanding that work like this can never be the outcome of a single person, I take this opportunity to express my profound sense of gratitude and respect to all those who helped me through the duration of this work.

I am highly grateful to the authorities of Thapar University, Patiala for providing this opportunity to carry out the thesis work.

I would like to express a deep sense of gratitude and thank profusely to my thesis guide, **Mr. J. S. SAINI** for their sincere & invaluable guidance, suggestions and attitude which inspired me to submit thesis report in the present form. His feedback and editorial comments were also invaluable for the writing of this thesis. I would also like to offer my sincere thanks to Mr. Tarun Nanda, Assistant Professor, Mechanical Engineering Department, Thapar University, Patiala for their everlasting support.

At last, I would like to thanks all the members and employees of Mechanical Department, Thapar University, Patiala for their intellectual support. My special thanks to my family members and friends who constantly encouraged me to complete this study.

Regards,

Ashish Mittal

(ASHISH MITTAL)

ABSTRACT

Metal cutting operations such as turning, milling and drilling are widely used in manufacturing to produce a variety of mechanical components. Drilling, a hole producing process, is especially important because it accounts for a large portion of overall machining operations. In addition, drilling problems can result in costly production waste because many drilling operations are usually among the final steps in fabricating a part.

The present study is focus on predicting the thrust force and torque in drilling using high speed drills, with different diameters, on the AISI 1020 steel. An analytical finite element technique is develop for predicting the thrust force and torque in drilling with twist drills. The approach is based on representing the cutting forces along the cutting lips as a series of oblique sections. Also the cutting in the chisel region is treated as orthogonal cutting with different cutting speeds depending on the radial location. For each section, an Eulerian finite element model is used to simulate the cutting forces. The section forces are combined to determine the overall thrust force and drilling torque on the drills. Results of predicted forces and torques are compared with measured forces and torques. The forces and torques predicted by the FEM are in close agreement with the experimental observed forces and torques in drilling tests of AISI 1020 steel for several drill diameters, spindle speeds and feed rates.

NOMENCLATURE

SYMBOLS	DESCRIPTION
A	: Area in the shear plane
b	: Cutting width
F_H	: Principal (cutting) force
F_t	: Friction force
F_T	: Transverse force
F_V	: Vertical (thrust) force
F_{tang}	: Force in transverse direction of drill
F_{thrust}	: Force in axial direction of drill
F_{rad}	: Force in radial direction of drill
i	: Inclination angle
L	: Pitch of the helix on the drill
N_t	: Normal force
Q	: Projected area of the cutting cross section
r	: Radius of the section from drill center
t	: Undeformed chip thickness
t_1	: Depth of cut
U_s	: Shear energy rate
U_f	: Friction energy rate
V	: Cutting velocity
V_c	: Chip flow velocity
V_s	: Chip velocity in the shear plane
w	: Half of the web thickness
α_e	: Effective rake angle
α_n	: Rake angle
α_s	: Side rake angle of tool
α_b	: Back rake angle of tool

C_s	: Side cutting angle of tool
β	: Friction angle
φ_e	: Shear plane angle, angle between the shear and cutting velocity
η_c	: Chip flow angle
ρ	: Half of the drill point angle
τ_s	: Shear stress in the shear plane

CONTENTS

LIST OF FIGURES

LIST OF TABLES

CHAPTER 1 INTRODUCTION

This chapter discusses the basic details and concepts of related topics associated with the thesis work.

1.1 DRILLING

Drilling is one of the most widely used methods of making holes. Drilling is the operation of making cylindrical holes into the solid geometry, Fig. 1.1 shows the drilling process.

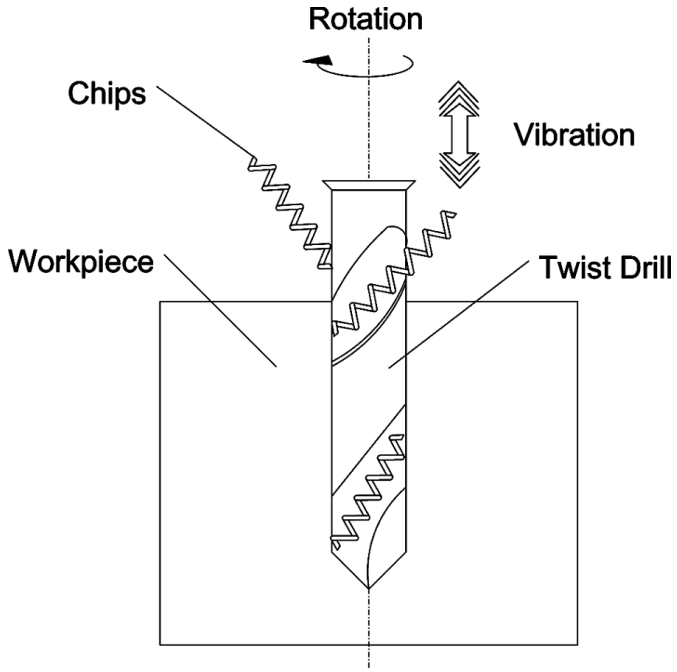

Figure 1.1 Drilling process

The cutting tool in this case is a drill with which a hole can be made from the solid or the diameter of a previously drilled hole can be increased (enlarging holes). The primary cutting motion in the drilling is rotary, a straight-line feed is used. In ordinary drill presses, both of these motions are imparted to the drill. The drill is clamped in the spindle which rotates it and feeds it downward into the workpiece clamped stationary into the table.

The same operation can also be used for other hole making operations such as center drilling, counter sinking and counter boring. This operation is limited to holes through the axis of rotation of the workpiece and form any of the ends.

The term *drill* can refer to a drilling machine, or can refer to a drill bit for use in a drilling machine. *Drill bit* or *bit* is used throughout to refer to a bit for use in a drilling machine and *drill* refers always to a drilling machine.

1.2 TWIST DRILL

Drill bits are cutting tools used to create cylindrical holes. Bits are held in a tool called a drill, which rotates them and provides torque and axial force to create the hole. Specialized bits are also available for non-cylindrical-shaped holes.

The twist drill bit is the type produced in largest quantity today. It drills holes in metal, plastic and wood.

The twist drill bit was invented by Steven A. Morse of East Bridgewater, Massachusetts in 1861.He received U.S. patent 38119 for his invention on April 7, 1863. The original method of manufacture was to cut two grooves in opposite sides of a round bar, then to twist the bar to produce the helical flutes. This gave the tool its name. Nowadays, the drill bit is usually made by rotating the bar while moving it past a grinding wheel to cut the flutes in the same manner as cutting helical gears.

The most common type of drill is a standard-point twist drill as shown in Fig. 1.2. This type of drill is versatile and can be used on a variety of materials such as wood, plastic, masonry, ceramic and metal. These drill bits have two spiral grooves running the length of the drill. These grooves aid in transporting cutting fluid to the drill tip and in removing the chips from the hole. These types of drill bits are held in chucks or collets on machines that are either hand-held or automated. This type of drilling can often cause burrs at both the entrance and the exit of the hole and parts often need a subsequent deburring operation to smooth out the holes.

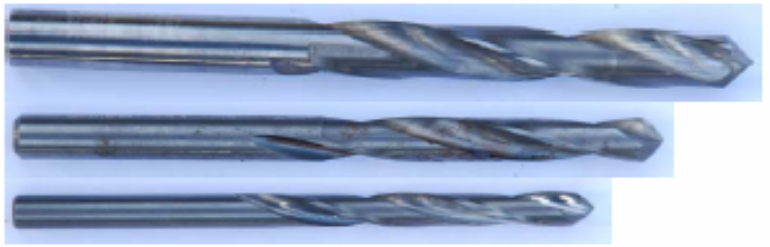

Figure 1.2 Twist drills

The geometry and sharpening of the cutting edges is crucial to the performance of the bit. Users often throw away small bits that become blunt and replace them with new bits because they are inexpensive and sharpening them well is difficult. For larger bits, special grinding jigs are available. A special tool grinder is available for sharpening or reshaping cutting surfaces on twist drills to optimize the drill for a particular material.

Tools recognizable as twist drill bits are currently produced in diameters covering a range from 0.05 to 100 mm (0.0020 to 3.937 inch). Lengths up to about 1,000 mm (39 inch) are available for use in powered hand tools.

Manufacturers can produce special versions of the twist drill bit, varying the geometry and the materials used, to suit particular machinery and particular materials to be cut. Twist drill bits are available in the widest choice of tooling materials. However, even for industrial users, most holes are still drilled with a conventional bit of high speed steel.

The most common twist drill (the one sold in general hardware stores) has a point angle of 118°. This is a suitable angle for a wide array of tasks and will not cause the uninitiated operator undue stress by wandering or digging in. A more aggressive (sharper) angle, such as 90°, is suited for very soft plastics and other materials. The bit is generally self-starting and cut very quickly. A shallower angle, such as 150°, is suited for drilling steels and other tougher materials. This style bit requires a starter hole but will not bind or suffer premature wear when a proper feed rate is used.

Drills with no point angle are used in situations where a blind, flat-bottomed hole is required. These drills are very sensitive to changes in lip angle and even a slight

change can result in an inappropriately fast cutting drill bit that will suffer premature wear.

1.2.1 Twist Drill Bit Geometry

The main geometry parameters of twist drill are described below, as shown in Fig. 1.3

- **Spiral:** The rate of twist in the drill, controls the rate of chip removal in a drill. A fast spiral drill is used in high feed rate applications under low spindle speeds, where removal of a large volume of swarf is required. Low spiral drills are used in cutting applications where high cutting speeds are traditionally used, and where the material has a tendency to gall on the drill or otherwise clog the hole, such as aluminum or copper.

- **Point angle:** The angle formed at the tip of the drill, is determined by material the drill will be operating in. Harder materials require a larger point angle, and softer materials require a sharper angle. The correct point angle for the hardness of the material controls wandering, chatter, hole shape, wear rate, and other characteristics.

- **Lip clearance angle** : The angle formed by the portion of the flank adjacent to the land and a plane at right angle to the drill axis measured at the periphery of the drill. The lip angle determines the amount of support provided to the cutting edge. A greater lip angle will cause the drill to cut more aggressively under the same amount of point pressure as a drill with a smaller lip angle. Both conditions can cause binding, wear, and eventual catastrophic failure of the tool. The proper amount of lip clearance is determined by the point angle. A very acute point angle has more web surface area presented to the work at any one time, requiring an aggressive lip angle, where a flat drill is extremely sensitive to small changes in lip angle due to the small surface area supporting the cutting edges.

- **Flank :** The surface on the drill which extends behind the cutting lip to the following flute is termed as flank.

- **Land or Margin :** It is the cylindrically ground body surface on the leading edge of the drill.

- **Rake Angle :** The angle between the tangent to the face (in the flute) at the point of the lip (cutting edge) being refereed to and the normal, at the same point, to the surface of revolution described by the lip about the drill axis.

The normal rake angle is highly negative near the chisel edge, the inclination angle is more positive.

- **Helix Angle :** The angle between the leading edge of the land and the axis of the drill. The large helix angle results in a more positive rake angle, which improves the cutting efficiency but also weakens the drill.

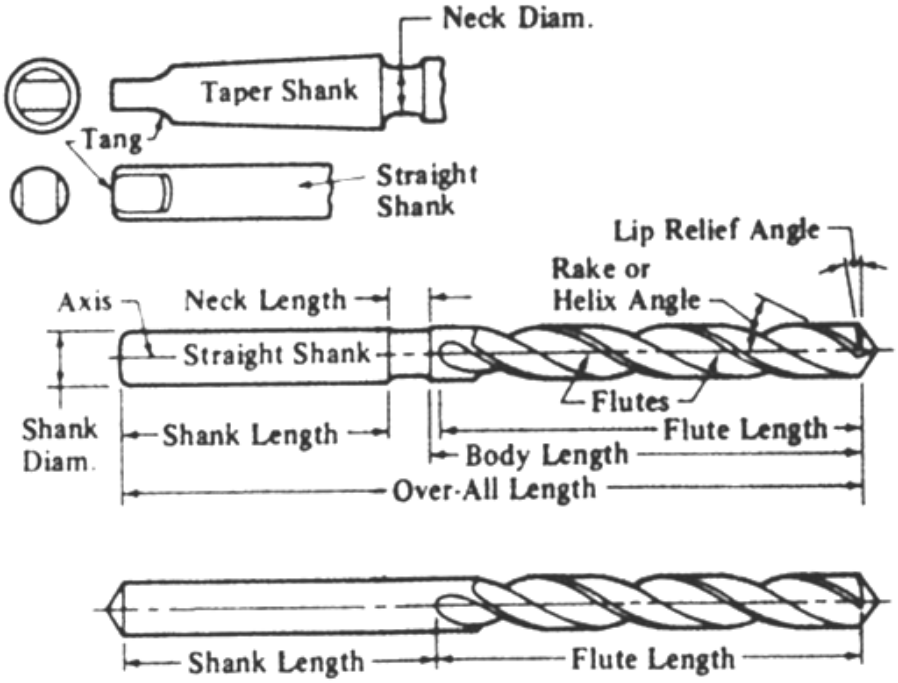

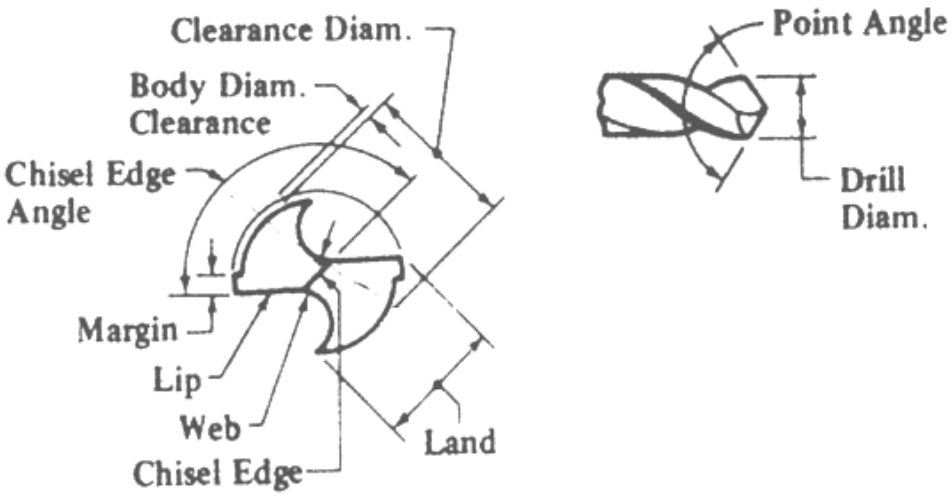

Figure. 1.3 Twist drill bit geometry

- **Lead of Helix:** The distance measured parallel to the drill axis, between the corresponding point on the leading edge of the land in one complete revolution.

- **Chisel Edge :** It is formed by the intersection of the two flanks. It provides the support during drilling and also provides drill point strength to resist lateral bending moments due to vibration or unbalanced forces during drilling. Cutting along the chisel edge is not efficient due to large negative rake angle and slow cutting speed near the centre of the drill. The cutting forces along the chisel edge contribute more than half of the total thrust force while only contributing a very small portion of the drilling torque.

- **Web :** The cutting edge is thickened gradually from the bottom, to provide the strength to the drill, is termed as web. The thrust force is maximum at the web where the material is compressed and extruded rather than sheared to the minimum value at the end of cutting edge.

Most drills for consumer use have straight shanks. For heavy duty drilling in industry, drills with tapered shanks are sometimes used.

1.3 ELEMENTS OF DRILL BIT GEOMETRY

Like a single-point tool, a drill has rake and relief angles.

The Rake angle, γ is the angle between the tangent to the face (in the flute) at the point of the lip (cutting edge) being referred to and the normal, at the same point, to the surface of revolution described by the lip about the drill axis.

The rake angle vary gradually along the lip. And it is measured in a plane perpendicular to the lip (plane *BB* in Fig.1.4). It can be determined (neglecting the thickness of the web) by the formula,

$$\tan\gamma_x = \frac{r_x \tan w}{R \sin\varphi} \qquad (1.1)$$

where

r_x = Radius of the circle on which the point being considered is located

R = Radius of the drill

w = Helix angle of the flutes

φ = One half of the point angle

The rake angle acquires its maximum value at the periphery of the drill where, in a plane parallel to the drill axis (plane *AA*), it is equal to the helix angle of the helix flutes.

The minimum value of rake angle is at the apex of the point. The rake angle at the chisel edge is negative so that the cutting angle exceeds 90° and the cutting conditions are unfavourable.

This marked variation of the rake angle along the whole length of the lip is an essential shortcoming of twist drills since it leads to the more complex conditions of the chip formation.

A larger rake angle, however, reduces the lip angle, leading to more rapid heating of this part of the drill and, consequently, to maximum wear.

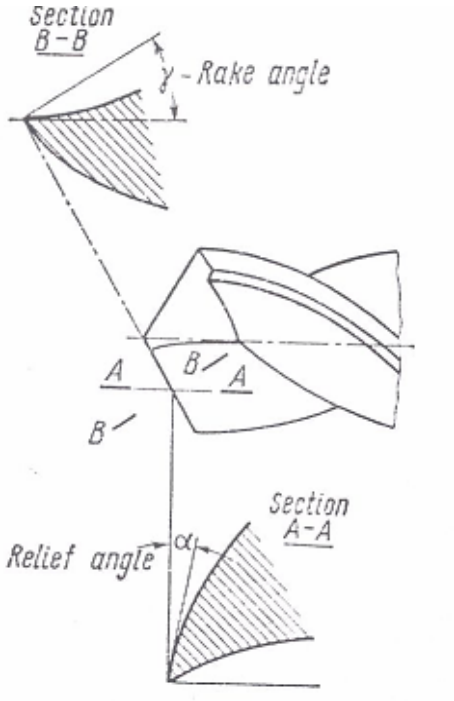

Figure 1.4 Rake and relief angles of a twist drill

The variation of the rake angle along the lip is evident from the graphical construction (Fig.1.5). If a helix is developed on a plane it will become the hypotenuse of the right triangle of which one side is lead (pitch) of the flutes and the other side is the circumference of the circle of a diameter on which the helix was formed.

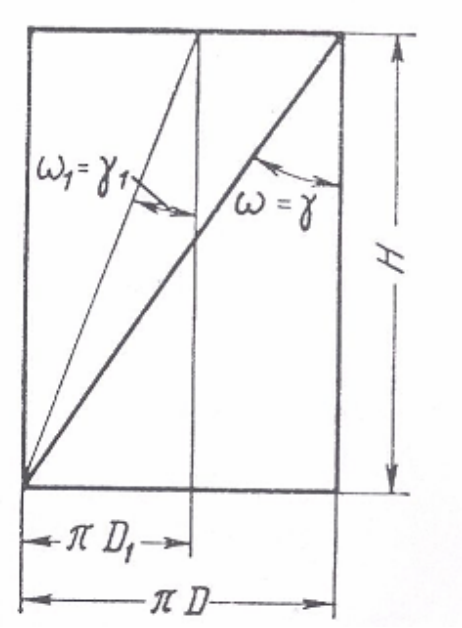

Figure 1.5 Variation in rake angle along the drill tip

The *relief angle,* α is the angle between a tangent to the flank, or lip relief surface, at the point being considered on the lip and a tangent at the same point to the circle the point describes as it rotates about the drill axis. This angle is measured in the plane *AA* which is which is tangent to the cylindrical surface (see Fig.1.4) on which the above mentioned tip lies. The axis of this cylindrical surface coincides with the drill axis.

The relief angle in a normal plane *BB* for a point on the periphery of the drill can be determined by the formula

$$\tan\alpha_x = \tan\alpha \sin\varphi \qquad (1.2)$$

The actual plane of cut is tangent to this helical surface. Hence, the actual relief angle in the process of drilling, the working-relief angle, α_w, is the angle between the actual plane of cut and a plane tangent to the lip relief surface of the drill.

The smaller the diameter of the circle on which the point being considered lies, the larger feed, *s*, the larger angle will be and smaller the working relief angles, α_w.

It can be seen from the drill geometry considered above that it has certain features which adversely influence the process of chip formation in drilling. These features include:

- Reduction in the rake angle along the lips as the point being considered approaches the drill axis.
- Unfavourable cutting conditions at chisel edge (since here cutting angle exceeds 90°).
- The lack of the relief angle on the margins, leading to increased friction in the drilled hole.

1.4 TOOL FORCES AND TORQUE ACTING ON DRILL

All the elements of a drill are subjected to certain forces in drilling. Resolving the resultant forces of resistance to cutting at each point of the lip we obtain three forces acting mutually perpendicular to each other.

The forces and torque in drilling are main parameters for efficient working of the drill. In drilling the force is divided into main three components, as shown in Fig. 1.6:

- Principal or cutting force (F_H): These horizontal forces acting on both lips in the radial direction cancel each other due to the symmetry of the cutting lips.

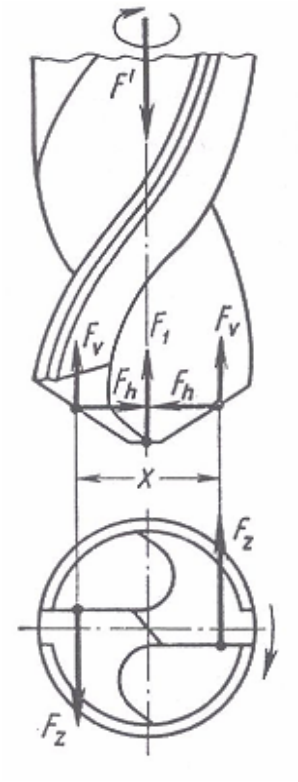

Figure 1.6 Forces acting on a drill

- Vertical component of force (F_V): This component of force acting in the axial direction of the drill contribute to the thrust force, acing upwards, impede the penetration of the drill into the work.
- Transverse component of force (F_T): This component of force used to predict the torque in drilling by multiplying this force with radial distance to the axis of the drill.

In order for the drill to penetrate into the work, the thrust force applied to it by the machine must overcome the sum of the forces of resistance acting along the drill axis. Thus

$$F^1 > \Sigma (2F_V + F_1 + F_f) \qquad (1.3)$$

It had been found from experiments that the forces of resistance F_V developed on the lips come to about 40 percent of the total resistance (thrust force F), the force of resistance developed on the chisel edge is about 57 percent and the friction forces F_f about 3 percent.

The forces which impede the advance of the drill into the material are overcome by the feed mechanism of the drill press whose design is based on the maximum axial thrust force, F .

In operating a drill press to given drilling conditions, it is necessary to see that the total force of resistance acting along the drill axis, or axial thrust force, F , is less or, in any case, equal to the maximum force F_{max} permitted by the feed mechanism (to avoid breaking the weakest link in the feed train), i.e. $F \leq F_{max}$.

The maximum permissible thrust force F_{max} is usually calculated when the machine is designed; it is given in the service manual or certificate of the machine tool.

Force, F_z sets up the moment of resistance

$$M_{rc} = F_z.x \qquad (1.4)$$

The total moment of forces of resistance is made up of the moment of forces F_z, moment of forces due to scraping and friction on the chisel edge, M_{ce}, moment of the friction forces on the margins M_m, and the moment of the forces of friction of the chip on the drill and on the machined surface, M_c.

Thus,

$$M = M_{rc} + M_{ce} + M_m + M_c \qquad (1.5)$$

Investigations show that about 80 percent of the total moment of the resistance to cutting is accounted for by the lips, 8 percent by the chisel edge and 12 percent by the friction between the chip and drill, chip and hole and the drill margins and the machined surface, (M_m + M_c).

In addition to the above mentioned condition concerning the penetration of the drill into the work, it will be necessary, in order to perform drilling in the given machine, that the total moment of resistance be overcome by the available torque of the drill press, i.e. $M_t \geq M$, the torque of the drill press is determined by the formula

$$M_t = 975{,}000 \frac{N_{sp}}{n} \quad \mathbf{kgf-mm} \qquad (1.6)$$

where

N_{sp} = Available power at the spindle, kW

n = Speed of the spindle (drill), rpm

Also,

$$N_{sp} = N_{mt} \cdot \eta \qquad (1.7)$$

where

N_{mt} = Power of the electric motor of the machine tool, kW

η = Efficiency of the machine tool

The total moment of resistance to cutting, M should not only be less or, in any case, equal to torque, M_t developed by the electric motor of the drill press at the given spindle speed, but also less or, at last, equal to the maximum torque, M_t^1 permitted by the weakest link in the main drive gear train (to avoid its breakage), i.e. $M \leq M_t^1$

Torque, M_t can be readily calculated by the formula given above, while torque, M_t^1 is generally calculated in designing the machine and is indicated in the service manual or certificate.

1.5 EFFECT OF VARIOUS FACTORS ON THE AXIAL THRUST AND TORQUE IN DRILLING

Drill torque and axial thrust are functions mainly on the following factors:-

1. Composition and hardness of the work material
2. Drill diameter and feed
3. Drill geometry

4. Cutting fluid efficiency
5. Drilling depth
6. Drill wear
7. Cutting speed

- **Workpiece Material:** The higher tensile strength or hardness of the material, the greater the axial thrust and the moment of the forces of resistance to cutting in drilling.

  This relationship can be expressed mathematically by the following equations:

  In drilling steels with high-speed steel drills,

$$F = C_1 \sigma_t^{0.75} \quad (1.8)$$

$$M = C_2 \sigma_t^{0.75} \quad (1.9)$$

  In drilling grey cast irons with carbide-tipped drills,

$$F = C_3 Bhn^{1.0} \quad (1.10)$$

$$M = C_4 Bhn^{0.5} \quad (1.11)$$

- **Drill diameter and Feed:** The larger the drill diameter and the rate of feed per revolution, the larger the cross sectional area of the undeformed chip will be, the greater the resistance of chip formation and, consequently, the greater the axial thrust and torque.

  Experimental research has indicated that the drill diameter has a greater effect in increasing F and M than the rate of feed. The reason is that the drill diameter seems to represent the depth of cut in drilling and, as such, has more influence on the forces acting in cutting than the feed.

- **Drill Geometry:** The *helix angle,* w of the flutes affects F and M in as much as it determines the rake angle of the drill. It follows from the formula, that the larger helix angle is, the larger rake angle will be at each point of the lip, the more easily the chip is formed.

$$\tan\gamma_x = \frac{r_x \tan w}{R \sin \varphi} \qquad (1.12)$$

Consequently, lower the axial thrust force, F and the moment of the forces of resistance, M as shown in Fig. 1.7, this reduction is more marked up to a value of 30°.

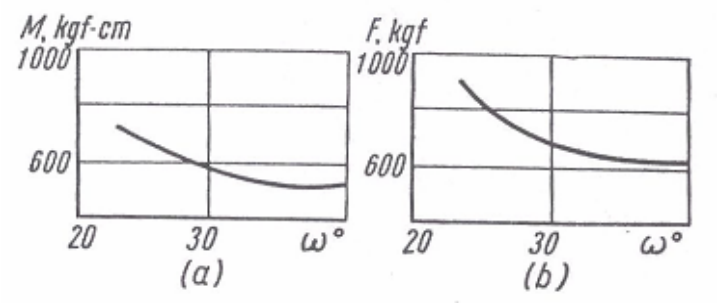

Figure 1.7 Effect of flute helix angle (a) on the torque, (b) on the axial thrust

The *point angle,* 2φ affects the ratio of the forces horizontal and vertical, as well as the undeformed chip thickness. Therefore, it cannot but affect thrust, F and torque, M upon reduction in the point angle, the horizontal forces increase and the vertical forces decrease in the same manner as both forces are changed upon a reduction of the plan approach angle of a single-point tool in turning, as shown in Fig. 1.8.

A reduction in vertical forces, in turn, leads to the reduction in the axial thrust force, F likewise, an increase in point angle leads to an increase in axial thrust force, F .

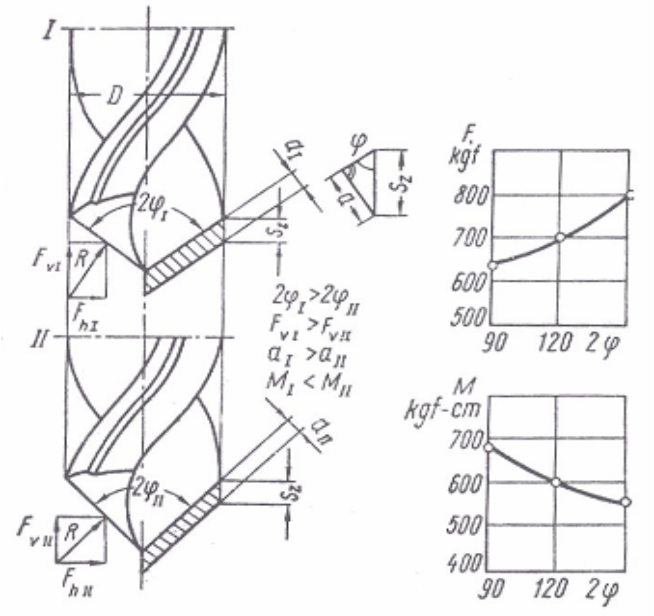

Figure 1.8 Effect of the point angle on the axial thrust and torque

- **Cutting- fluid efficiency:** The favorable action of cutting fluids is manifested in drilling as well since the cutting process in drilling is accompanied by the same phenomena as in turning. Consequently, the use of suitable cutting fluids and especially surface-active emulsions, leads to a reduction in the axial thrust (feeding force) and the torque, in comparison with drilling dry, by 10 to 30 percent for steel, 10 to 18 percent for cast iron and 30 to 40 percent for aluminum alloys.

- **Drilling Depth:** The cutting conditions deteriorate with an increase in the depth of the hole being drilled. Difficulties are encountered with cutting fluid delivery and chip ejection; heat evolution is increased, as is the degree of work-hardening. All of these factors reduce the drill life and increase the axial thrust and torque. Cutting at a great depth can be facilitated by grinding chip breaker grooves on the drill which divide the chip, making it easier to eject, and reduce the heat generation, axial thrust and torque.

- **Drill Wear:** With the increase in the flank wear of the drill (on the lip relief surface), as shown in Fig. 1.9, F and M are increased. In comparison with a sharp drill, the use of a dull drill raises F and M by 10 to 16 percent.

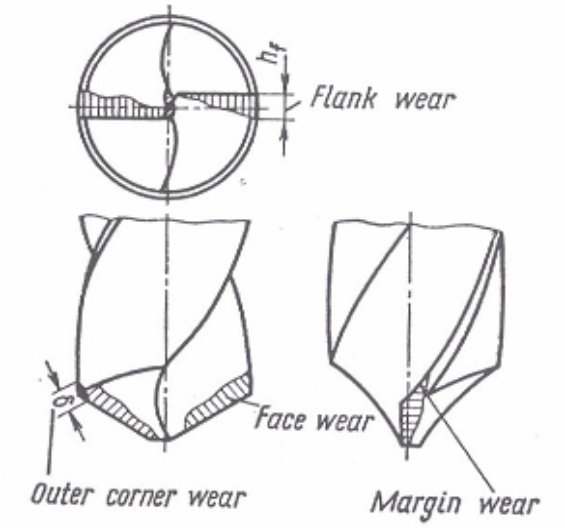

Figure 1.9 Wear of high-speed steel twist drill

- **Cutting Speed:** Axial thrust, F and torque, M are first increased and then decreased with an increase in the cutting speed. This effect of the cutting speed is reduced with an increase in the feed and, beginning with speed 0.4 mm per rev, the cutting speed has practically on effect of F and M .

1.6 FINITE ELEMENT METHOD (FEM)

In Finite Element Method, a complex region of defining a continuum is discretized into simple geometric shapes called 'Elements'. The material properties and the governing relationships are considered over these elements in term of unknown values at element corner. An assembly process, duly considering the loading and constraints, results in a set of equations which are solved for results.

The Finite Element Method has become a very powerful tool for the numerical solution of a wide range of application. The application ranges from deformation & stress analysis of automotive parts, aircraft, building & bridge structures etc. Finite Element Method not only give the behavioral insight of the different part of the structure but it also analyze the structure taking the individual behavior of these parts into consideration

and because of this fact it is becoming popular with the engineering field. It is also the trend in the industry that results are acceptable only when solved using certain computer programs. The following section discusses elementary information about Finite Element Methods.

1.6.1 Brief History

Basic idea of the Finite Element Method originated from advances in aircraft structure analysis. Turner derived stiffness matrices for truss, beam and other elements and presented their findings in 1956. in the early 1960s, engineers used the method of approximate solution of problem in stress analysis, fluid flow, heat transfer and other areas. A book by Argyris in 1955 on energy theorems and matrix methods laid a foundation for further developments in Finite Element studies. The first look on Finite Element by Zienkiewicz and Chung was published in 1967. In the late 1960s and early 1970s, Finite Element Analysis was applied to non linear problems and large deformation. Oden's book on non linear continua in 1972, mathematical foundations were laid in 1970s. Today's the developments in mainframe computers and availability of powerful microcomputer have brought this method within reach of students and engineers working in small industries.

1.6.2 Basic Steps of Finite Element Method

Finite Element Method can be divided into several distinctive steps. Theoretical approach to the method and its different steps are as follows:

- **Discretization**

Discretization is the process of dividing the domain of problem into small regions or sub-domains known as 'Elements'. Corner points of the elements are called 'Nodes'. Some of most usual elements of 1D is line, of 2D are triangles, quadrilaterals and of 3D are tetrahedrons, hexahedrons, pentahedrons.

- **Element Analysis/ Element Stiffness Matrix**

The Element analysis has two key components, expressing the variable within the elements and maintaining equilibrium of the elements.

The governing equation is converted to algebraic form which is represented in matrix form and is called Element equation or Element stiffness matrix. This enables solution by computer. Element stiffness matrix represents the response of elements according to its property in the system for parameters. Same matrix can be used for all elements of same type. Following steps are used for conversion of governing equation (differential or integral) into algebraic form.

- **Construction of Trail Solution:-** It is a cyclic process by hit trail. The equation with certain Degree of freedom (DOF) is taken, which is solved by applying boundary condition either at the starting for manual processing or after formulation of system stiffness matrix for solution through computer.

- **Application of Optimization Criteria:-** Optimization criteria are used to find the values of trail function. Various methods used for optimization are given below
  - Method of weighted residual
  - Collocation method
  - Sub domain method
  - Least square method
  - Galerkin method
  - Ritz variational method

- **Estimation of Accuracy:-** The accuracy of solution is checked for closeness to exact solution. Also accuracy can be checked by checking the reducing difference of the consecutive solutions obtained by increasing degree of freedom known as property of Convergence.

  Sources of error in FEM are:-
  - Domain error: Discretization of domain is approximate.
  - Computational error: Integration and differentiation induce error.
  - Approximation error: Assumption of DOF makes the solution approximate.

- **System Analysis/ System Stiffness Matrix**

The matrix equations for the individual elements are combined to form the matrix equations for the entire system called System stiffness matrix. It gives the response of the parameters on the entire system.

- **Incorporation of Boundary and Loading Conditions**

The system stiffness matrix is modified according to the overall boundary conditions. This reduces calculation work and saves time.

- **Solving to System Equations**

The system equations can be solved to give the unknown values at the nodes. If the problem is of equilibrium nature, then the obtained by solving a set of linear or non-linear equations. System equations can be solved by number of available solvers like Gauss Elimination or Gauss Siedel etc.

- **Post Processing/ Display**

The Post processing stage deals with the representation of results. Typically, the deformed configuration, mode shapes, temperatures and stress distribution are displayed at this stage.

CHAPTER 2 LITERATURE REVIEW

A lot of research work has been carried out throughout the world for predicting the thrust force and torque in drilling. A brief review of literature is being presented here.

2.1 LITERATURE REVIEW

Williams [1] constructed a model of chip formation and an indentation model for the chisel edge region of a twist drill. From these models, predictions were made as to the shape of the wear zone about the chisel edge and equations derived for calculating the torque and thrust developed by the chisel edge given the geometry of the drill point, the cutting conditions and a shear stress factor for the work material. Using the chisel edge thrust equation, it was shown that as the drill feed tends to zero, the drill thrust approached a finite value, the magnitude of which was in reasonable agreement with that observed experimentally.

Armarego and Cheng [2] developed a cutting analysis, based on oblique cutting models, for the drill lips of flat rake face drills. The analysis was predicting the reasonable deformation and force distributions along the drill lips. An analysis for conventional drills was also attempted with less success. The concept of geometrical similarity was studied and found be useful for prediction of forces in drilling and for the design of twist drills.

Armarego and Cheng [3] predicted the effect of geometrical similarity on the deformation and forces of different sized conventional and modified drills experimentally. The flat rake face drill considerably reduced the forces in drilling. The cutting analysis for the lips of modified drills were found to be qualitatively and quantitatively sound. Statistical methods were used to process the data and verify the theoretical predictions.

Watson [4] predicted the torque and thrust in drilling by the cutting lips was developed from an oblique machining model that a number of individual elements can represent the material being machined by each lip.

Watson [5] modified the previous model **[4]** which assumed a series of elements across the cutting lip and underestimated the torque and thrust, to account for the necessary integrity of the chip. Because the integral chip flows initially as a unit in one direction and was rotating about a point, there must be a linear variation in the chip velocity across the lip. That variation in chip velocity affects the shear angle across the lip, effectively reducing the range from that calculated for a series of elements. When that extra work of effectively holding the various elements together was taken into account, predictions much closer to the experimental results were obtained. The modified model accounted reasonably for variation of most of the drill and process variables.

Watson [6] developed a model to indicate that on the region adjacent to the centerline, material was cut in a normal machining process by the rake face and extruded under the clearance flank when the working clearance angle was positive. As the radius increased, the feed angle decreased and the working clearance angle changed from negative to positive, while the working rake angle changed from a positive (about 30°) to a large negative value (-60°). When the magnitude of the negative rake angle becomes greater than 45°, it was unlikely that machining will occur, and because of that a metal removal process akin to a wear process was proposed for this region.

Watson [7] performed full drill tests to confirm the chisel edge model that incorporated wear, extrusion and cutting regimes revealed that, in contradiction to previous information, variation of the cutting speed was produced a great change in the thrust. An explanation of these results were advanced in terms of the dynamic strain ageing response of the material when the material to be machined was at an elevated temperature because of the unsteady heat transfer from the heat source on the cutting at the chisel edge.

Agapiou and DeVries [8] described the analytical temperature distributions along the cutting edge and on the flank face of a twist drill. The analysis was based on the assumption that the material being machined by the drill lips can be represented by a series of concentric elements. The technique was used to obtain a steady state solution while a transient solution evolved from a closed-form approach to a semi-infinite solid had a constant surface heat flux. The theoretical approach also identified important physical quantities, such as the absorption coefficient of the work material, which affect the cutting temperatures.

Agapiou and DeVries [9] evaluated the analytical models, for estimating the temperature distributions along the cutting edge and on the clearance face of a twist drill, using an experimental technique that measures average drill flank temperatures. While the transient model tends to overestimate the values of the average flank temperatures, especially during drilling to a one diameter hole depth, the temperatures predicted from the steady state model agreed reasonably well with the experimental results. The difference between the analytical and experimental results varied with the physical and thermal properties of the powder metallurgy work materials used in this experiment.

Stephenson and Agapiou [10] described a model for calculating main cutting edge torque, thrust and radial force distributions for drilling gray cast iron with solid carbide and carbide-tipped drills. A general parametric method for characterizing complex point geometries was first described. Together with empirical cutting force models from end cutting tests, torque, thrust and radial force calculations were carried out for ten representative drills covering a range of available geometries. Calculated and measured torque values agreed to within the repeatability of the measurements. Calculated thrust force values were reasonable but were significantly lower than measured values in most cases, since chisel edge contributions were not included. Calculated radial forces for an asymmetric drill agree with limited measured values to within twice the repeatability of the measurements.

Rubenstein [11] conducted drilling operations with a set of geometrically similar twist drills to relating the torque and the thrust to feed and drill diameter in previously derived

expressions. The model from which the theoretical expressions were derived was showed to be capable of explaining the apparently deviant behaviour observed when drilling workpieces which exhibit high adhesion. The model was based on the assumption that the removal process at the drill lips was quasi-orthogonal which was valid provided the drill diameter was sufficiently large compared to the chisel edge length. The behaviour observed with small diameter drills was showed to be consistent with the removal process becoming noticeably oblique.

Chandrasekharan *et al.* [12] developed models to predict the thrust and torque forces at the different regions of cutting on a drill. The mechanistic approach adopted to develop these models exploits the geometry of the process, which was independent of the workpiece material. The models were calibrated to a particular material using the well established relationships between chip load and cutting forces, modified to take advantage of the characteristics of the drill point geometry. The cutting-lips model predictions agreed well with the experimental data for both materials, the chisel-edge model proposed for metals agreed well with the experimental data.

Chandrasekharan *et al.* [13] developed model to predict the forces for arbitrary drill point geometry. The cutting lips were divided into elements and the elemental forces were determined from a fundamental oblique cutting model. The method developed to parametrically defined the cutting lip in three-dimensional space and to determined the oblique cutting parameters (cutting angles and chip thickness) at each element on the cutting lip. The model did not require calibration experiments for each point geometry. Here the conical drill was used to determine the model coefficients for a tool and workpiece material combination and these were used for other drill point geometry.

Min *et al.* [14] introduced the advance understanding of the burr formation process, a series of finite element models. First, a finite element model of the burr formation of two-dimensional orthogonal cutting was introduced and validated with experimental observations. A detailed and thorough examination of the drilling burr forming process undertaken. This information was used in the construction of an analytical model and,

leads to development of a three dimensional finite element model of drilling burr formation and related burr formation problems that had not been physically examined can be simulated and the results used to control process planning resulting in the reduction of burr formation.

Shatla and Altan [15] analyzed both the drilling and ball end milling operations using analytical modeling. The cutting edges of the twist drill lip and the ball end mill were divided into oblique cutting elements that had geometries and cutting conditions that vary with the location of the element on the cutting edge. The analysis was performed for each element using flow stress data and thermal properties of the workpiece material, tool geometry and cutting conditions. Predicted temperatures on the flank side of the twist drill lip and predicted ball end milling force results were compared with the experimental data.

Bono and Ni [16] developed a model to predict the effects of thermal distortion of the drill and workpiece on the diameter and cylindricity of dry drilled holes. Experiments using embedded thermocouples verify that the model predicts the flow of heat into the workpiece and into the drill reasonably well. The model predicted that thermal expansion of the drill was the dominant effect and leads to oversized holes with diameters that increase with depth.

Bono and Ni [17] developed a model for predicting the heat that flows into the workpiece during dry drilling processes. The measured drilling thrust and torque were used as inputs in an oblique cutting analysis, and an advection heat partition model was developed to calculate heat flux loads on a finite element model of the workpiece. Experiments using embedded thermocouples had verified that the model accurately predicts the temperature field in the workpiece for a range of drilling speeds and feeds.

Strenkowski *et al.* [18] developed model of three-dimensional cutting for predicting tool forces and the chip flow angle. The approach consists of coupling an orthogonal finite element cutting model with an analytical model of three-dimensional cutting. The finite element model was based on an Eulerian approach, which gave excellent agreement with

measured tool forces and chip geometries. The analytical model in which a minimum energy approach was used to determine the chip flow direction. The model required orthogonal cutting test data to determine the tool forces and chip flow angle. With this approach, a predictive model of three-dimensional cutting can be developed that did not require measured data as input. Cutting experiments were described in which good agreement was found between measured and predicted tool forces and chip flow angles for machining of AISI 1020 steel.

Carroll and Strenkowski [19] described two computer models that treated the special cases of orthogonal cutting. The models were based on the finite element method, which was used to discretize a portion of the workpiece in the vicinity of the cutting tool. The detailed stress and strain fields in the chip and workpiece, chip geometry and tool forces can be determined from the models. The first model was based on a specially modified version of a large deformation updated Lagrangian code developed at Lawrence Livermore National Laboratory, which employs an elastic-plastic material model. The second model treats the region in the vicinity of the cutting tool as an Eulerian flow field. Material passing through the field was modeled as viscoplastic. Results obtained from both models showed excellent agreement when compared with measured tool forces for slow speed cutting of aluminium 2024-T361.

Strenkowski and Moon [20] predicted a model for chip geometry and temperature distribution in the workpiece, chip, and tool without the need for empirical cutting data. With the capability to predict chip geometry the tool-chip contact length also be found. Characteristics of the flow field in the vicinity of the tool also be determined such as the material velocity, the stress and strain-rate distributions. It was found that the shear stress occurs over a finite region in front of the tool, rather than a single shear plane. Cutting experiments were performed for aluminum alloy 6061-T6 to validate the model. Good correlation with the model was found based on tool forces and average tool-chip interface temperature measurements.

Athavale and Strenkowski [21] described model for predicting the chip breakability potential of groove and obstruction-type tools. The potential for a tool to break chips was

evaluated in terms of the chip geometry and the damage sustained by the chip as it was formed in the shear zone. The chip geometry was characterized by its thickness-to-radius ratio and the material damage was evaluated in terms of a normalized accumulated damage factor that was based on a hole growth and coalescence model and was evaluated using a finite element cutting model. A total of 210 cutting tests were conducted to verify the model. Different tools including flat, obstruction and groove were tested for cutting of AISI 1020 steel and SS 304 steel. Each of these tool geometries exhibited significantly different chip thickness-to-radius ratios and normalized accumulated damage. Threshold criteria for breaking chips were determined for chosen steels. For difficult-to-break materials such as stainless, a lower normalized accumulated damage was needed and a higher chip thickness-to-radius ratio was required to break chips. Although the model presented was developed for orthogonal cutting, it can be readily extended to three dimensional machining processes.

Shih [22] developed the plane-strain finite element method and applied to model the orthogonal metal cutting of annealed low carbon steel with continuous chip formation. Four sets of simulation results for cutting with -2°, 0°, 5°, and 15° rake angle were summarized and compared to analyze the effects of rake angle in the cutting processes. The initial and deformed finite element meshes, as the cutting reaches steady-state condition were first presented. Simulation results of the cutting forces and residual stresses along with the X-ray diffraction measurements of the residual stresses generated using a worn cutting tool with 5° rake angle, were used to identify the influences of the rake angle and tool sharpness. Elements were selected to represent three sections along the shear and contact zones and under the cut surface. The normal and shear stresses distributions of parameters along these three sections, and contours of temperature, plastic strain, and effective stress were then presented.

Bono and Ni [23] developed a drill-foil thermocouple system for measuring the temperature distribution along the cutting edges of a drill. The system was simple to implement and it did not suffer the problems experienced by previously developed methods. The drilling processes cause twist drills to reach extreme temperatures, which

can have severe effects on the quality of holes produced and on the life of the tools. This study develops a method for measuring the temperature distribution along the cutting edges of a drill. Experiments show that the method was accurate, produced repeatable measurements and was sensitive to the drilling conditions including the speed, feed and drill geometry.

Strenkowski *et al.* [24] developed an analytical finite element technique for predicting the thrust force and torque in drilling with twist drills. The approach was based on representing the cutting forces along the cutting lips as a series of oblique sections. For each section, an Eulerian finite element model was used to simulate the cutting forces and then the section forces were combined to determine the overall thrust force and drilling torque.

From the literature review it can be seen that the Finite Element studies are useful when used in conjunction with an experimental testing program. Predicting the thrust force and torque in drilling using Finite Element Analysis allows for a more extensive parametric investigation of the underlying behavior than is possible in a laboratory setting. In previous years, much progress has been made in the Finite Element modeling of the thrust force and torque in drilling. Finite Element modeling of experimental specimens allows for a better understanding of forces and the torque in the drill and to better investigate their influence on drill.

CHAPTER 3 FEM FORMULATION

From the literature review discussed in the previous chapter, it is seen that FEM can be used to model the specimen for the better understanding of forces and torque in the drilling process. In the present work an analytical model for oblique cutting is described for analyzing a single section in the cutting lip region of the drill, which can be combined to determine the thrust force and torque. The model is developed using the Eulerian Finite Element with Minimum Energy Approach.

These approaches are given below:-

Minimum Energy Approach: This approach helps to find the chip flow angle. The angle is found from the condition that, the chip flow in a direction to minimize the cutting energy.

Total cutting rate (U) = Shear energy rate on the shear plane (U_s) +
Friction energy rate on the tool face (U_f)

Eulerian Finite Element Approach: An Eulerian Finite Element Technique is well suited for modeling steady state cutting processes. In this method, the workpiece and chip flow through a control volume defined by the Finite Element grid. The chip shape is established by requiring that external boundaries of the chip be coincident with the assumed chip boundaries.

The main advantage of this approach is that it can be used to model chip formation with negative rake angles and both the forces and the heating of the drill due to plastic work and friction can be integrated in a single model to predict forces and drill temperatures as a function of workpiece, feed and speed.

3.1 SINGLE EDGE OBLIQUE CUTTING MODEL

The cutting action along the cutting lips in a drill can be interpreted as occurring within a series of oblique sections, in which the rake and inclination angles vary radially along each lip [2,3]. In this paper, an analytical finite element technique was adopted for

predicting the chip flow angle and three-dimensional oblique cutting forces that occurs in each section [18]. The technique was based on a minimum energy approach as developed by Strenkowski *et al.* [24] for determining the chip flow angle. An Eulerian model developed by Strenkowski *et al.* [18] was coupled with this minimum energy approach for the orthogonal cutting force data. The model developed is shown below.

Consider first the simplest case of a tool with an oblique cutting edge as shown in Fig. 3.1, which has been adapted from Strenkowski *et al.* [24]. The inclination angle of the main cutting edge is i , the depth of cut is t_1 and the cutting width is b . The underlying assumption is that a chip is produced by shear forces acting in the plane *CJFD* with the main cutting edge CD .

Three-dimensional cutting can be interpreted as a collection of plane strain orthogonal cutting slices. One typical plane is represented by *IHERQGC*, which is cross-hatched in Fig. 3.1.

This plane is defined by the cutting velocity, V and the chip flow velocity vector, V_c . Chip formation in this plane may be regarded as plane strain deformation with a corresponding shear angle, mean friction angle, and work material shear strength as in orthogonal cutting.

Therefore, line CE may be regarded as coincident with the shear plane and line HI may be considered to be the undeformed chip thickness in orthogonal cutting. Any other plane that is parallel to the plane *IHERQGC* will have the same effective shear plane angle and effective rake angle, but with a different depth of cut, t.

Therefore, three-dimensional cutting is interpreted as a series of orthogonal slices, each with the same effective shear plane angle and effective rake angle along the main cutting edge.

The effective rake angle is measured in the plane formed by the chip flow velocity, V_c and cutting velocity, V and it is defined by the angle between the chip flow direction and a line normal to the cutting velocity. This angle can be related to the chip flow angle, inclination angle, i and rake angle by

$$\alpha_e = \sin^{-1}(\sin\alpha_n \cos\eta_c \cos i + \sin\eta_c \sin i) \qquad (3.1)$$

The chip flow angle, η_c can be determined by using a minimum energy approach.

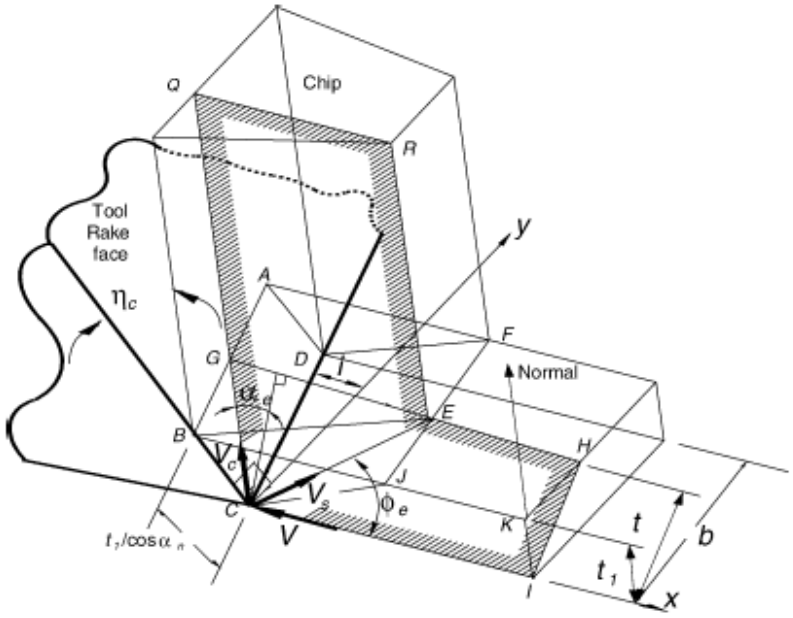

Figure 3.1 Model of Oblique Cutting

The total cutting energy rate consists of the shear energy rate (U_s) on the shear plane and friction energy rate (U_f) on the tool face. The shear energy rate, U_s can be expressed as:

$$U_s = \tau_s A\, V \qquad (3.2)$$

where τ_s is the shear stress in the shear plane and V_s is the shear velocity in the shear plane.

The area of the shear plane area of *CJFD* is A, which is equal to the cross-product of the vectors CE and CD, as shown in Fig. 3.1. An orthogonal coordinate system with origin at point *C* is defined as shown in this figure. The x-axis is defined along line *CI* and parallel to the cutting velocity vector, V. The y-axis is in the plane determined by V and the tool edge CD. The angle between the y-axis and line CD is i. The z-axis, not shown in Fig.3.1, is perpendicular to the x- and y-axes to form a right-handed coordinate system.

Also the length of lines CG and HI are given by,

$$CG = \frac{t_1}{\cos\alpha_n \cos\eta_c}$$

and

$$HI = \frac{t_1 \cos\alpha_e}{\cos\alpha_n \cos\eta_c}$$

Vectors CE and CD can be expressed as:

$$CE = \left[\frac{t_1 \cos\alpha_e}{\cos\alpha_n \cos\eta_c \tan\varphi_e}, \sqrt{\left(\frac{t_1 \cos\alpha_e}{\cos\alpha_n \cos\eta_c}\right)^2 - {t_1}^2}, t_1\right]$$

and $$CD = [-b \tan i, b, 0]$$

The area A is equal to the cross-product $CE \times CD$, which can be rearranged as:

$$A = b\sqrt{{t_1}^2(1 + \tan^2 i) + z^2} \qquad (3.3)$$

where

$$z = \frac{p}{\tan\varphi_e} + \sqrt{(p^2 - {t_1}^2)} \tan i \qquad (3.4)$$

$$p = \frac{t_1 \cos\alpha_e}{\cos\alpha_n \cos\eta_c} \qquad (3.5)$$

Based on orthogonal cutting theory, velocity in the shear plane is given by

$$V_s = \frac{\cos\alpha_e}{\cos(\varphi_e - \alpha_e)} V \qquad (3.6)$$

where φ_e is the angle between the shear plane and cutting velocity and α_e is the effective rake angle.

Thus the shear energy rate, U_s in Eq. (3.2) can be rewritten as

$$U_s = \frac{\tau_z A \cos\alpha_e}{\cos(\varphi_e - \alpha_e)} V \qquad (3.7)$$

Similarly, the friction energy rate, U_f on the rake face can be written as,

$$U_f = F_t \frac{\sin\varphi_e}{\cos(\varphi_e - \alpha_e)} V \qquad (3.8)$$

where F_t is the friction force on the rake surface.

In order to calculate the total energy rate from Eqs. (3.7) and (3.8), the effective shear plane angle (φ_e) and the shear plane stress (τ_s) must be known.

It is assumed that the relationships between φ_e and τ_s and the effective rake angle, α_e are the same as those in orthogonal cutting under equivalent conditions. In addition, by assuming that the friction force acting on a unit width of the tool face with undeformed chip thickness (t) is the same as the friction force in orthogonal cutting with unit width of cut and undeformed chip thickness (t), the friction force F_t can be written as

$$F_t = \frac{\tau_s \sin\beta \cos\alpha_e}{\cos(\varphi_e + \beta - \alpha_e)\sin\varphi_e} Q \qquad (3.9)$$

where β is the friction angle on the tool face and Q for a sharp nose tool can be written as

$$Q = \frac{bt_1}{\cos\alpha_n \cos i} \qquad (3.10)$$

Eqs. (3.9) and (3.10) are used to calculate the friction energy rate, U_f.

The total cutting energy rate can be found by adding the contribution from the shear and friction energy rates. Note that the energy rates are dependent on the chip flow angle, η_c which is not known. However, the angle can be found from the condition that the chip will flow in a direction that minimizes the cutting energy, U .

Based on the minimum cutting energy, the tool force components can be derived from geometric considerations

$$F_H = N_t \cos\alpha_n \cos i + F_t \sin\alpha_e \qquad (3.11)$$

$$F_V = -N_t \sin\alpha_n + F_t \cos\eta_c \cos\alpha_n \qquad (3.12)$$

$$F_T = -N_t \cos\alpha_n \sin i + F_t \sin\eta_c \cos i - F_t \cos\eta_c \sin i \sin\alpha_n \qquad (3.13)$$

where F_H, F_V and F_T are the principal (cutting), vertical (thrust) and transverse components of the tool force, respectively and N_t and F_t are the normal and friction forces that can be determined once the minimum energy is known. The force components are functions of α_n, i , b, t_1 and η_c which are known constants, except for the chip flow

angle, η_c which can be evaluated by minimizing the cutting energy. Therefore the three-dimensional tool forces can be readily determined.

In the analysis, orthogonal cutting tests are necessary to provide the shear stress, τ_s, shear angle, φ_e, and friction angle, β needed in the above equations. As an alternative, an Eulerian finite element cutting model is used to determine the orthogonal cutting data [18].

3.2 DRILLING MODEL

The analytical finite element oblique cutting technique described in the previous section is applied to selected sections along the cutting lip to determine the drilling forces. At each oblique cutting section, the three-dimensional cutting forces are calculated and then combined to determine the drilling thrust force and torque. The geometry of a typical twist drill as defined in terms of three key parameters, the helix angle (δ), point angle (2ρ) and web-thickness (2ω). Both the helix angle and the point angle will affect the rake angle along each cutting lip. A large helix angle results in a more positive rake angle, which improves the cutting efficiency but also weakens the drill.

3.2.1 Cutting Lip Force Model

For the drilling model, each cutting lip is divided into oblique cutting sections for which the corresponding three-dimensional forces can be determined. For each section, the rake and inclination angle must be determined. For straight cutting lips, the inclination angle, i and normal rake angle, α_n can be determined by the following formula:

$$\sin i = \frac{\omega \sin \rho}{r} \tag{3.14}$$

$$\tan \alpha_n = \cos i \left(\tan \alpha_s \cos C_s + \tan \alpha_b \sin C_s\right) \tag{3.15}$$

where

$$\tan \alpha_s = \frac{\tan \delta}{\tan C_s} - \frac{\tan i}{\sin C_s} \tag{3.16}$$

$$\cos C_s = \frac{\cos\rho}{\cos i} \tag{3.17}$$

$$\tan\alpha_b = 2\pi\frac{r}{L} \tag{3.18}$$

$$\delta = \tan^{-1}\left(\frac{2\pi r}{L}\right) \tag{3.19}$$

In Eqs. (3.14) to (3.19), ω is the half web thickness, r is the radial distance from the drill axis, L is the pitch length of the helix on the drill, α_s is the side rake, α_b is the back rake and C_s is the side cutting angle of tool.

Using the single edge oblique cutting model, forces in the horizontal, vertical, and lateral directions can be determined. Note that forces are based on a local coordinate system for each section along each cutting lip. These local forces must be transformed to the global coordinate system corresponding to the radial, axial, and transverse directions of the drill.

Forces in the axial direction contribute to the thrust force. The torque consists of the transverse force times the radial distance to the axis of the drill. The forces in the radial direction cancel each other due to the symmetry of the cutting lips.

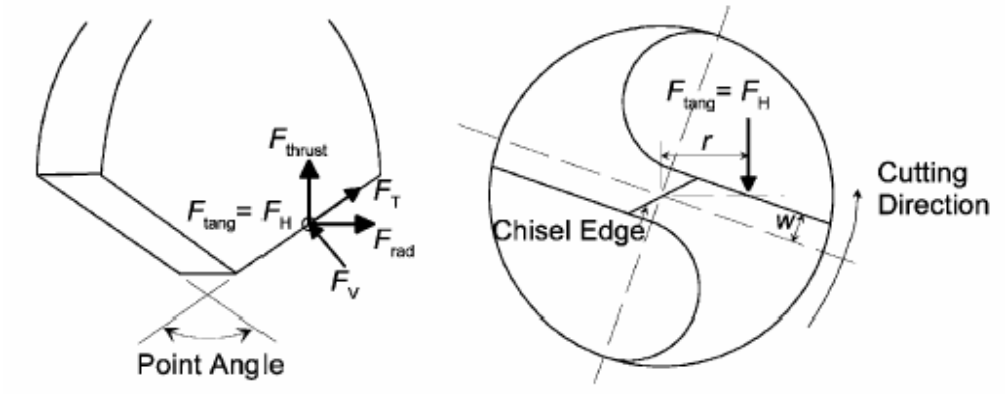

(a) Side view **(b) Top view**

Figure 3.2 Conversion of F_H, F_V and F_T in oblique cutting to F_{tang}, F_{thrust} and F_{rad} on a drill

Fig. 3.2 shows the directions of the local (F_H, F_V, F_T) forces and global force components (F_{tang}, F_{thrust}, F_{rad}) for a typical radial location along a drill cutting lip.

The equations for transforming local oblique cutting forces to the global drill coordinates are:

$$F_{tang} = F_H \quad (3.20)$$

$$F_{thrust} = F_T \cos\rho + F_V \frac{\sqrt{(r^2 - w^2)}}{r} \sin\rho \quad (3.21)$$

$$F_{rad} = F_T \frac{\sqrt{(r^2 - w^2)}}{r} \sin\rho - F_V \cos\rho \quad (3.22)$$

Generally, the cutting edges in a drill are curved and not necessarily straight as shown in Fig. 3.2. Only certain combinations of the helix angle, point angle and radius of flute can produce a straight cutting lip.

3.2.2 Chisel Edge Force Model

The majority of the material removed by a drill occurs from the cutting action of the cutting lips. In contrast, the chisel edge provides support during drilling. Cutting along the chisel edge is not efficient due to the large negative rake angle and the slow cutting speed near the center of the drill. The cutting forces along the chisel edge typically contribute more than half of the total thrust force, while only contributing a very small portion of the drilling torque. Although the chisel edge removes little material, it plays an important role in providing drill point strength to resist lateral bending moments due to vibration or unbalanced forces during drilling.

Cutting within the chisel edge region can be treated as equivalent orthogonal cutting slices. The cutting speed for each slice depends on the distance from the centerline. The cutting speed varies from nearly zero at the center of the drill to its maximum at the transition with the cutting lip.

For a typical drill with a 118° point angle, the rake angle for an orthogonal section in the web region is -59°. Cutting under such a negative rake angle is very difficult to model with an updated-Lagrangian finite element formulation [22]. However, an Eulerian approach can be successfully applied for orthogonal cutting with large negative rake angles, as long as the mesh is carefully designed.

CHAPTER 4 RESULTS AND VALIDATION

4.1 GENERAL

The purpose of the present work is to investigate the thrust force and torque in drilling for different drill diameters. An analytical finite element technique, as discussed in previous chapter, was developed for predicting the thrust force and torque in drilling with twist drills. The experimental tests were carried out using Drilling Machine using a High Speed Steel Twist Drill to validate the results.

4.2 FEM FORMULATION

The FEM formulation discussed in previous chapter was applied to selected section along the cutting lip to determine the drilling force. The FEM drilling model is based on representing the drill point geometry as a series of oblique sections. An analytical model for oblique cutting was first used to analyze a single section in the cutting lip region of the drill. Results of these sections were then combined to determine the thrust force and torque for various operating conditions. The geometry of a typical twist drill, defined in terms of the key parameters, the helix angle, point angle and web-thickness as shown in Fig.4.1.

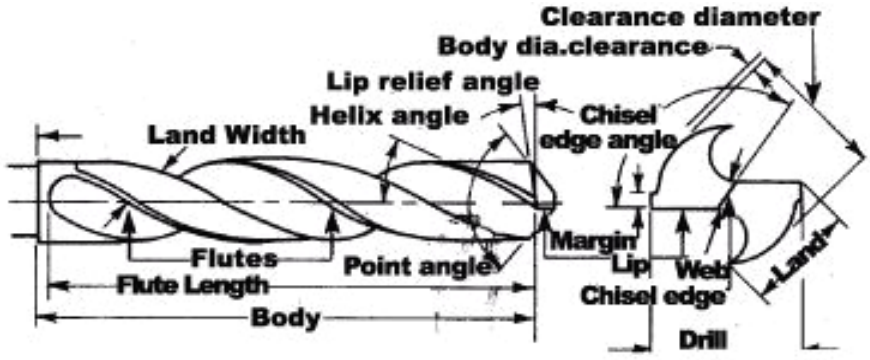

Figure 4.1 Twist drill with helix angle, point angle and web thickness.

Both the helix angle and point angle affects the rake angle along each cutting lip. The majority of the material removed by a drill occurs from the cutting action of the cutting lips. The chisel edge provides support during drilling. Cutting along the chisel

edge is not efficient due to the large negative rake angle and the slow cutting speed near the center of the drill. The cutting forces along the chisel edge typically contribute more than half of the total thrust force, while only contributing a very small portion of the drilling torque. Although the chisel edge removes little material, it plays an important role in providing drill point strength to resist lateral bending moments due to vibration or unbalanced forces during drilling.

Cutting within the chisel edge region can be treated as equivalent orthogonal cutting slices. The cutting speed for each slice depends on the distance from the centerline. The cutting speed varies from nearly zero at the center of the drill to its maximum at the transition with the cutting lip.

For a typical drill with a 118° point angle, the rake angle for an orthogonal section in the web region is -59°. The approach discussed in previous chapter can be successfully applied to orthogonal cutting with large negative rake angles.

Firstly, the mesh was generated with quadrilateral elements using C language. The mesh generated for orthogonal cutting with a -59° rake angle as shown in Fig. 4.2. Both the workpiece and the cutting tool are included in the model.

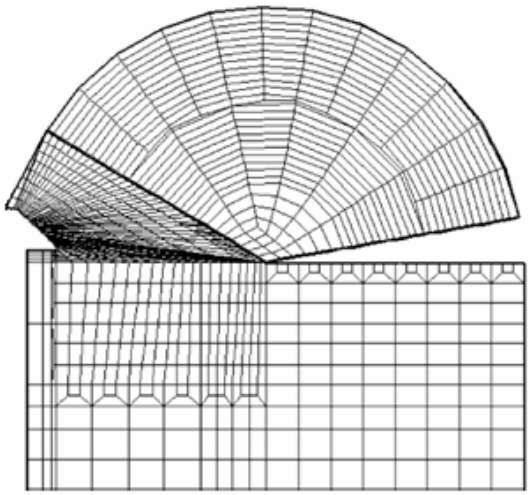

Figure 4.2 Finite element mesh for a -59° negative rake angle for the web of a drill with 118° point angle.

In the Finite Element model, five sections were used to represent each cutting lip and four sections were used to model the chisel edge. Table 1 lists the geometry of each section for a twist drill with a 12.7 mm diameter, 30° helix angle, 118° point angle drill,

1.70 mm web thickness and 302 rpm spindle speed. For each section, Table 1 lists the radial location of the section, the cutting speed, depth of cut, width of cut, inclination angle, rake angle, chip flow angle and effective rake angle. It can be seen from Table 1 that, from the outer to the inner drill radius, the effective rake angle decreases and the inclination angle increases for each section which indicates that the cutting action is becoming more oblique. Throughout the chisel edge region, orthogonal conditions are in effect so that the inclination angle is zero and the rake angle has a large negative value. For drilling of AISI 1020 steel, the forces for each section are also shown in Table 1. As expected, the radial force, F_{rad} is zero in the chisel edge region.

Table 1: Sections of oblique cutting for drilling

r (mm)	Cutting speed, V (mm/s)	Depth of cut, t_1 (mm)	Width of cut (mm)	Inclination angle, i (°)	Rake angle, α_c (°)	Chip flow angle, η_c (°)	Effective rake angle, α_e (°)	F_{tang} (N)	F_{rad} (N)	F_{thrust} (N)	Torque, $F_{tang} \cdot r$ (N-mm)
5.82	183.9	0.051	1.04	7.7	28.3	1	28.2	95.1	30.2	39.6	554
4.78	151.1	0.051	1.04	8.8	22.3	4	22.9	100	32.9	40.4	476
3.73	118.1	0.051	1.04	11.3	15.1	6	16.0	107	36.1	43.9	398
2.69	85.1	0.051	1.04	15.7	6.0	11	8.7	118	42.0	49.3	318
1.63	51.3	0.051	1.04	26.6	-8.6	21	2.0	143	57.3	57.0	233
0.97	30.5	0.051	0.28	0	-59.0	0	-59.0	35.9	0.0	64.5	34.8
0.69	21.6	0.051	0.28	0	-59.0	0	-59.0	35.9	0.0	64.5	24.8
0.41	13.0	0.051	0.28	0	-59.0	0	-59.0	35.9	0.0	64.5	14.7
0.14	4.3	0.051	0.28	0	-59.0	0	-59.0	35.9	0.0	64.5	5.03

After applying the formulation, the finite element predicted principal, vertical and transverse forces using 0.13 mm/rev feed and 0.80 m/sec cutting speed for five inclination angles are as shown in Fig. 4.3.

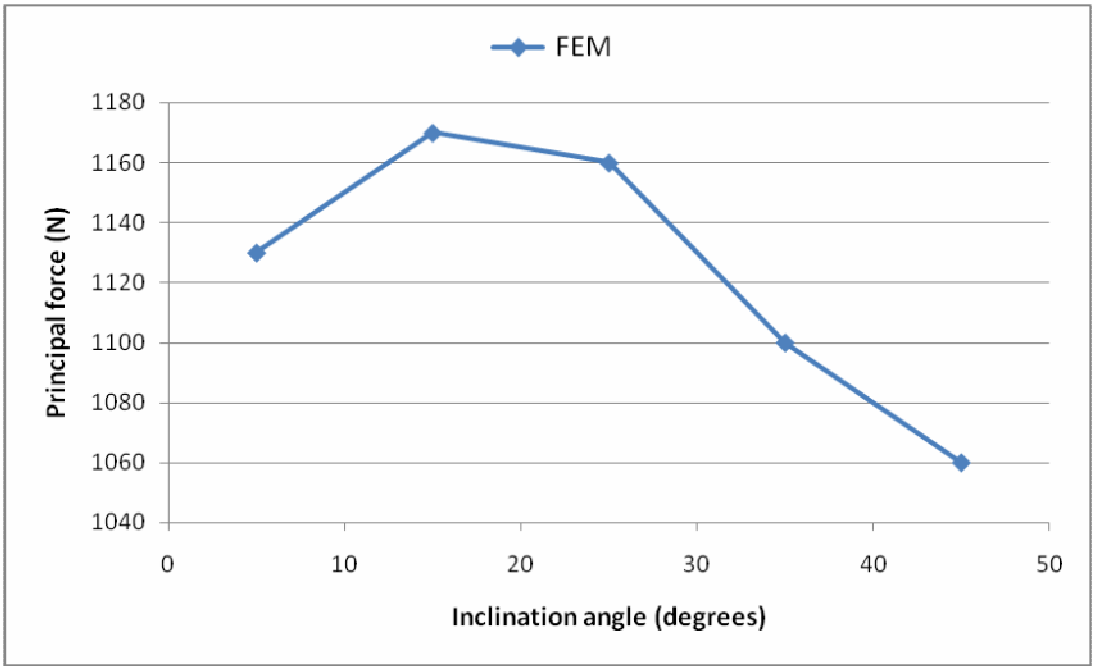

(a) Principal force

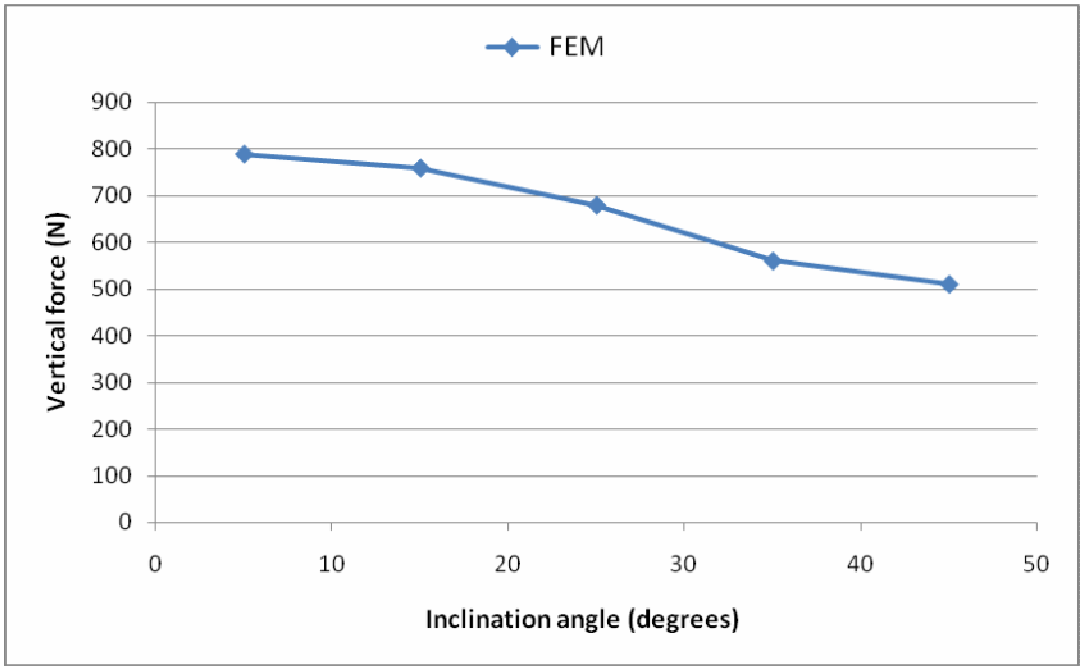

(b) Vertical force

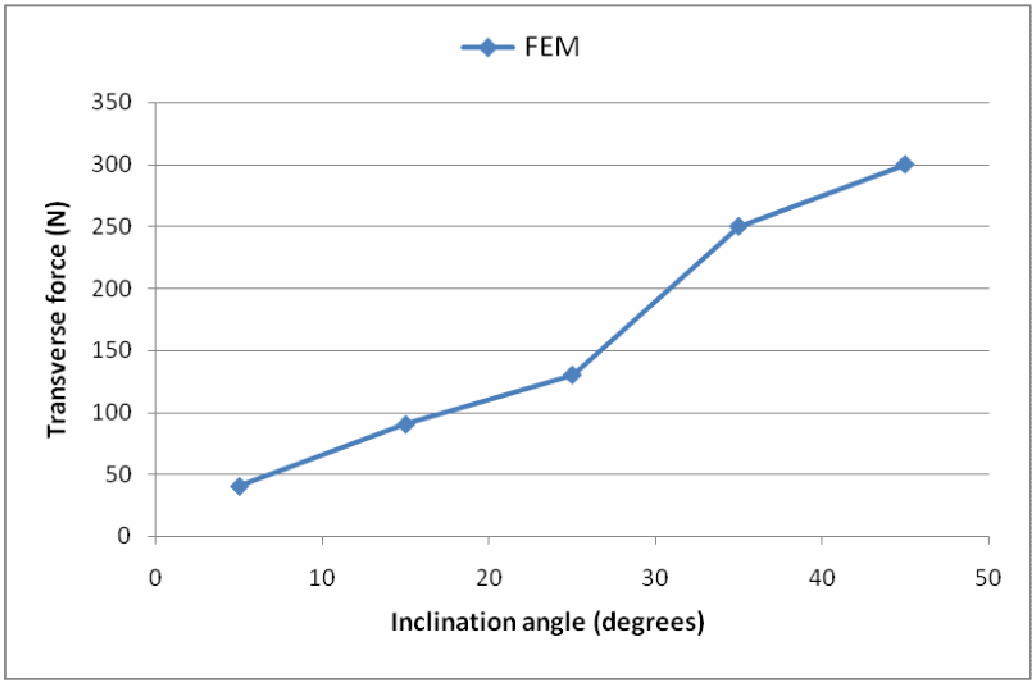

(c) Transverse force

Figure 4.3 The finite element predicted forces for five inclination angles

The finite element predicted thrust force in nine drilling tests i.e., with three drills with 6.35, 9.53 and 12.7 mm diameters and three feed rates of 0.051, 0.076 and 0.102 mm/rev are as shown in Fig.4.4.

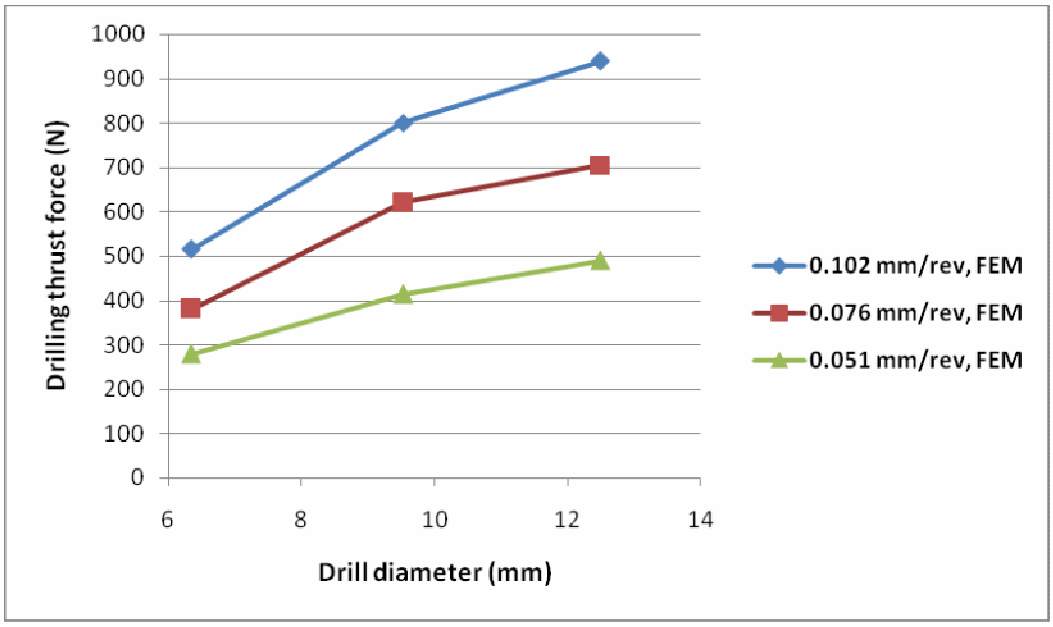

Figure 4.4 The finite element predicted thrust forces in nine drilling tests

4.3 EXPERIMENTAL VALIDATION

The drilling tests were performed on a drilling machine using a high speed steel twist drill with a 30° helix angle and 118° point angle. The workpiece was an AISI 1020 steel block. A spindle speed of 302 rpm was used. These drills with 6.35, 9.35 and 12.7 mm diameters were used for these feed rates. For all the tests, a peizo-electric three component force dynamometer (Kistler, Type 5070A) was used to measure the cutting, drilling forces and torque. The block diagram along with the actual experimental set up and peizo-electric three component force dynamometer (Kistler, Type 5070A) are as shown in Fig. 4.5.

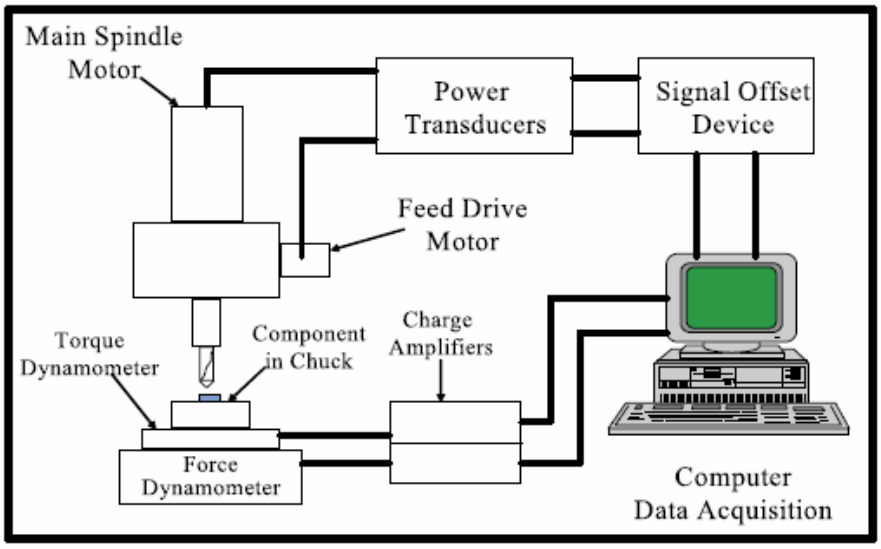

(a)

(b)

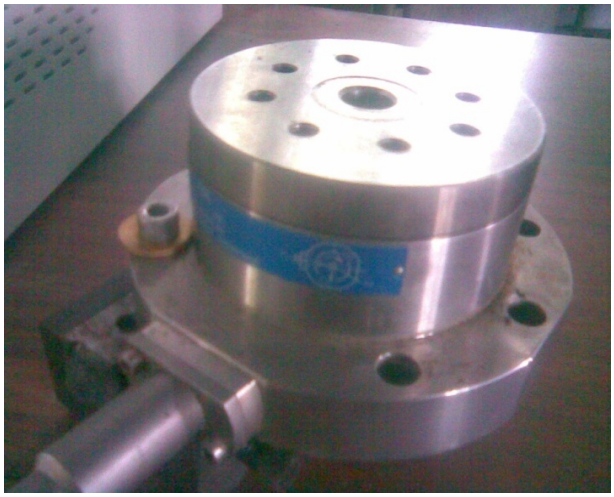

(c)

Figure 4.5 (a) Block Diagram, (b) Equipment set-up
(c) Piezo-electric three-component dynamometer (Kistler, Type 5070A)

The experimental measured principal, vertical and transverse forces using 0.13 mm/rev feed and 0.80 m/sec cutting speed for five inclination angles are as shown in Fig. 4.6.

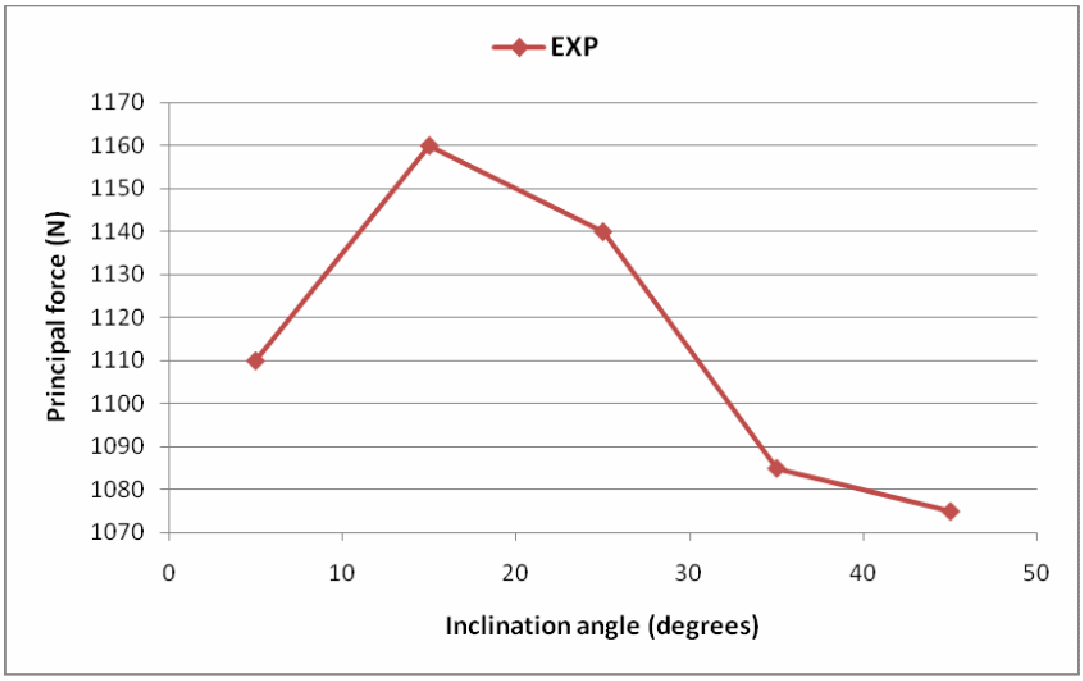

(a) Principal force

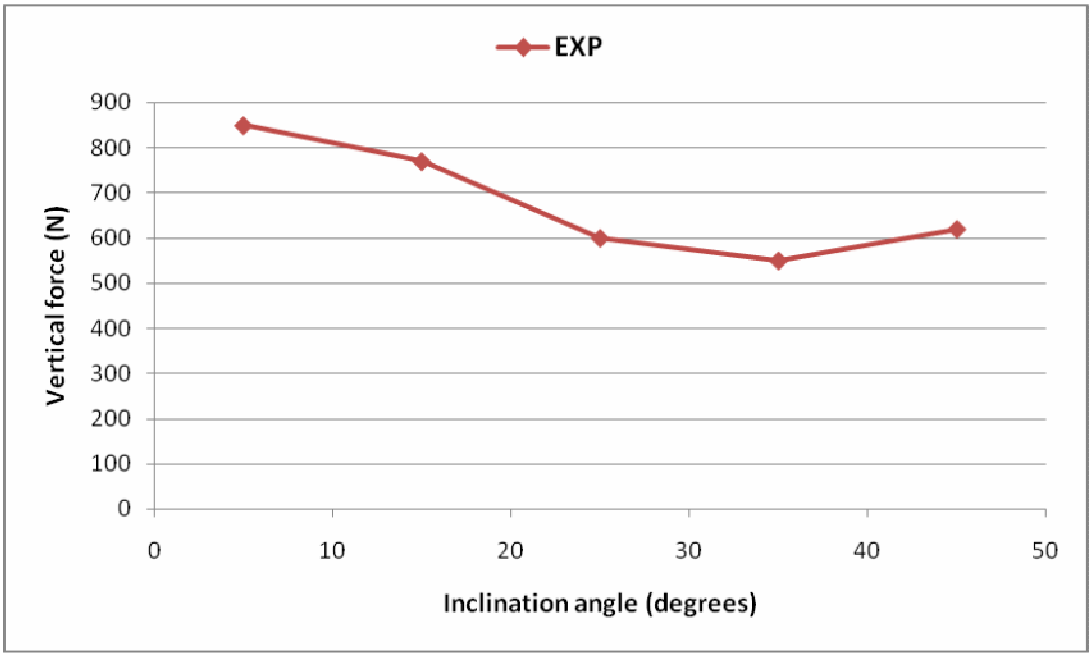

(b) Vertical force

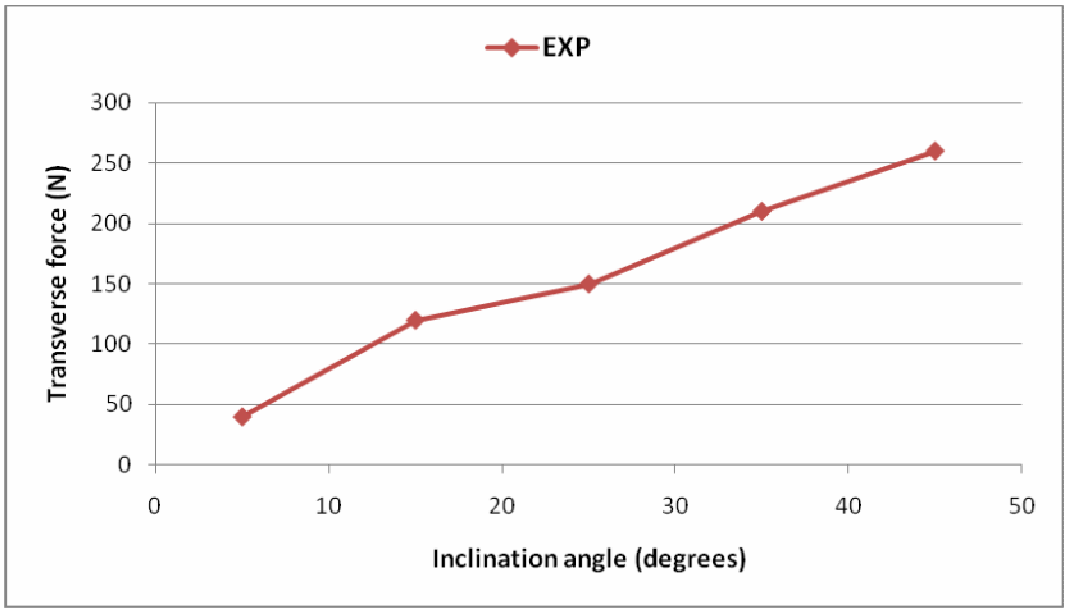

(c) Transverse force

Figure 4.6 The experimental measured forces for five inclination angles

The experimental measured thrust force in nine drilling tests i.e., three drills with 6.35, 9.53 and 12.7 mm diameters and three feed rates of 0.051, 0.076 and 0.102 mm/rev are as shown in Fig.4.7.

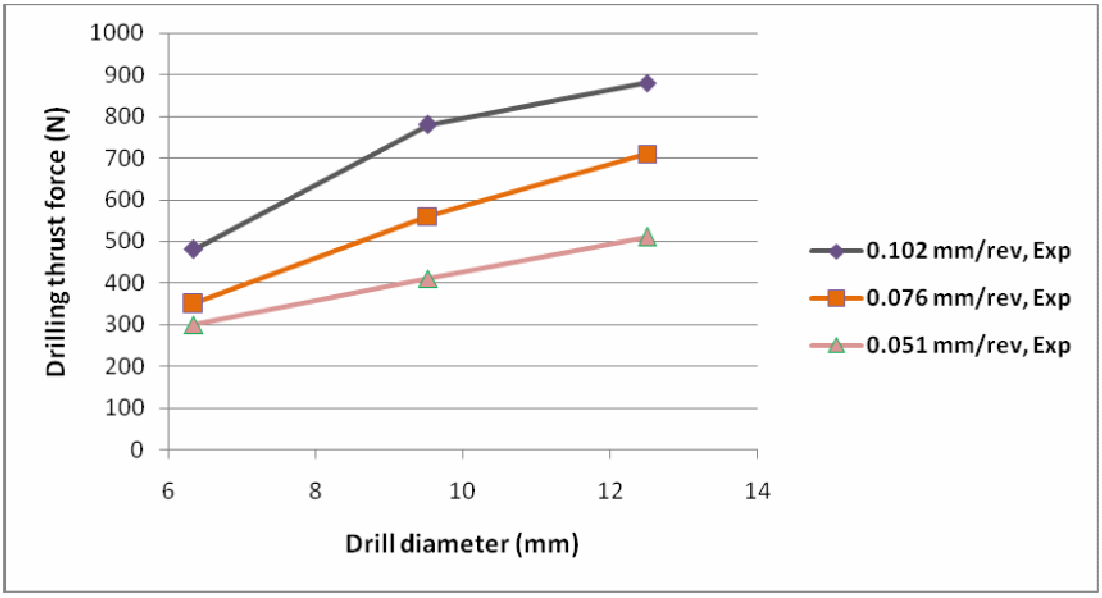

Figure 4.7 The experimental measured thrust forces in nine drilling tests

A comparison of the analytical and experimental forces are shown in Fig. 4.8 and Fig. 4.9. Very good agreement for the drilling forces were observed.

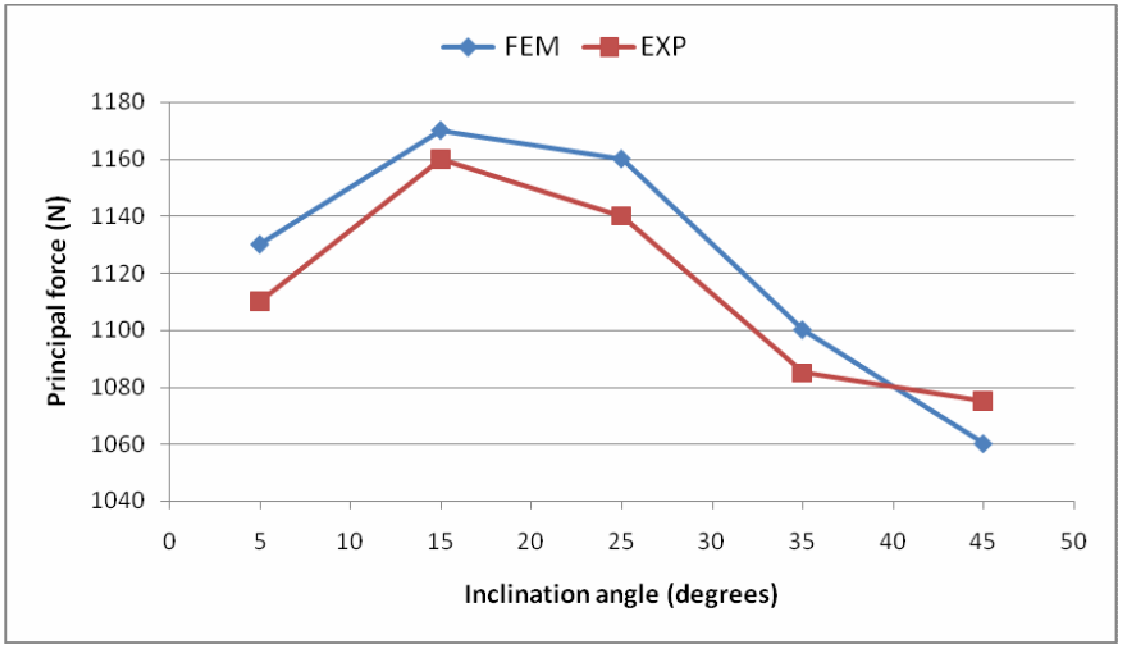

(a) Principal force

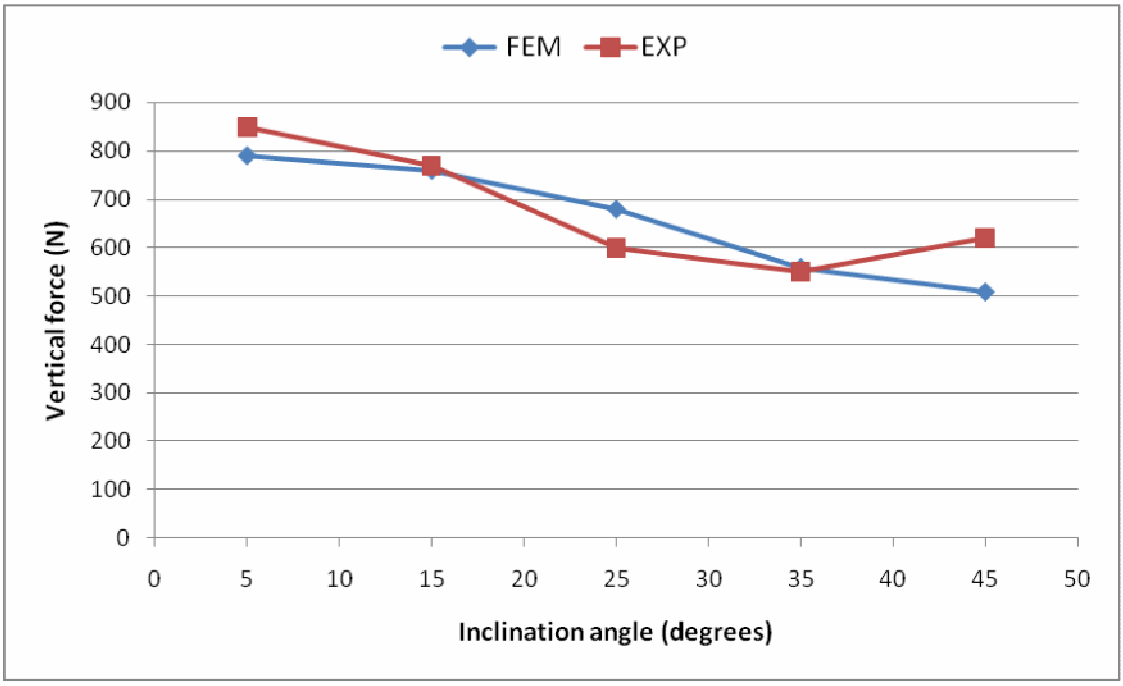

(b) Vertical force

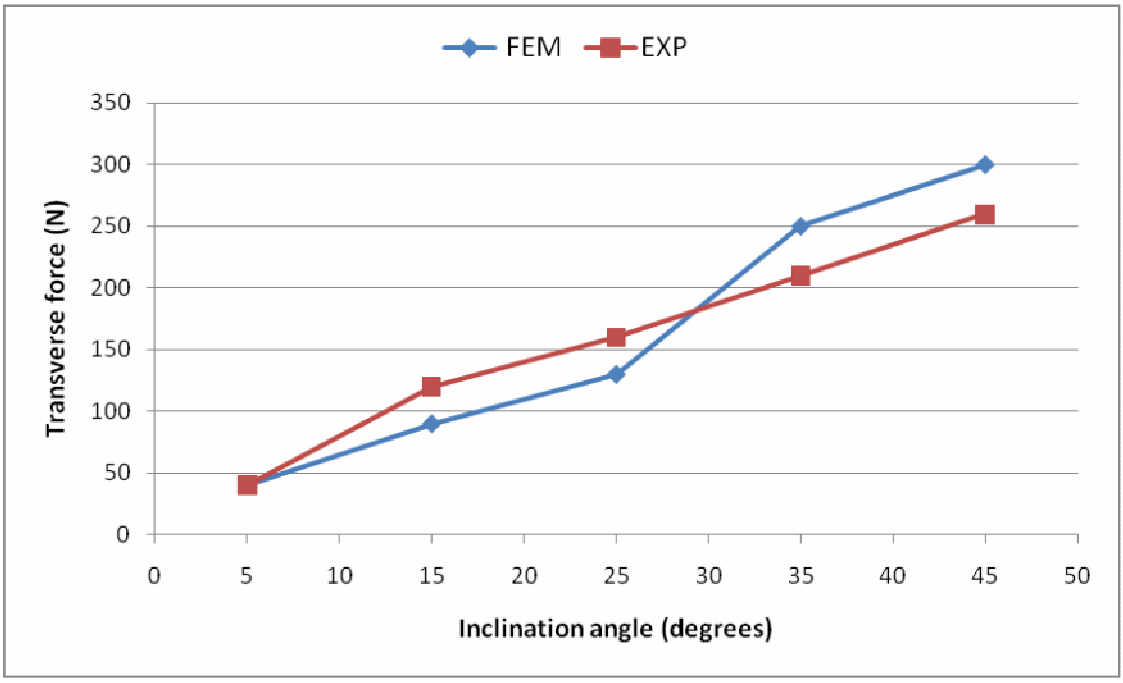

(c) Transverse force

Figure 4.8 The finite element predicted and experimental forces for five inclination angles

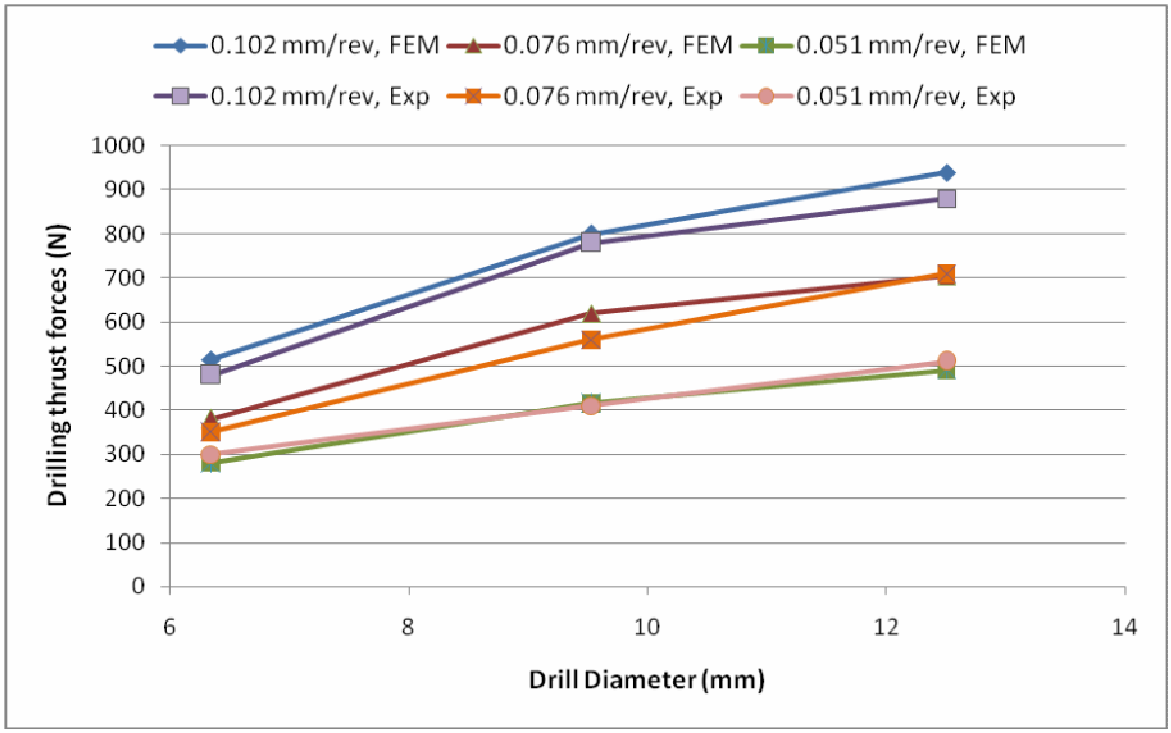

Figure 4.9 The finite element predicted and experimental thrust forces in nine drilling tests

The cutting force components that comprise the thrust force are also used to calculate the torque. Therefore, it is reasonable to assume that since good agreement was found between the analytical and experimental thrust forces, good agreement would also occur between the analytical and experimental torques. Table 2 shows the comparison between the analytical and experimental torques.

Table 2: Comparison of predicted and measured thrust force and torque

Drill diameter (mm)	Torque (Nm)		Thrust force (N)	
	Analytical	Experimental	Analytical	Experimental
6.35	1.61	1.81	735	775
9.53	3.47	3.51	1040	1070
12.7	6.17	5.88	1380	1440

The good agreement between the measured and predicted values for both the thrust forces and torques further validates the analytical finite element formulation.

CHAPTER 5 CONCLUSION

5.1 CONCLUSION

An analytical finite element technique was developed for predicting the thrust force and torque in drilling with twist drills. The approach was based on representing the cutting forces along the cutting lips as a series of oblique sections. Similarly, cutting in the chisel region was treated as orthogonal cutting with different cutting speeds depending upon the radial location. For each section, a finite element model was used and was combined to determine the overall thrust force and torque. The results were then validated with the experimental test preformed. Good agreement between the predicted and measured forces was found.

The model is applicable to general drill geometries, under different workpiece material and cutting condition. It can be readily applied to non-conventional drills other than standard twist drills as the formulation is independent of any specific drill geometry.

5.2 SCOPE FOR FUTURE WORK

The technique can be applied to predict drill tip temperature, which is an important indicator of drill life. Heat flux from each oblique and orthogonal section can be determined and then used to calculate the temperature distribution throughout the drill.

REFERENCES

[1] R. A. Williams, "A study of the basic mechanics of the chisel edge of a twist drill", *International Journal of Production Research*, vol. 8, pp. 325-343 (1970).

[2] E.J.A. Armarego and C.Y. Cheng, "Drilling with flat rake face and conventional twist drills-I. Theoretical investigation", *International Journal of Machine Tools and Manufacture,* vol. 12, pp. 17-35 (1972).

[3] E.J.A. Armarego and C.Y. Cheng, "Drilling with flat rake face and conventional twist drills-II. experimental investigation", *International Journal of Machine Tools and Manufacture*, vol. 12, pp. 37-54 (1972).

[4] A.R. Watson, "Drilling model for cutting lip and chisel edge and comparison of experimental and predicted results. I-initial cutting lip model", *International Journal of Machine Tool Design and Research,* vol. 25, pp. 347-365 (1985).

[5] A.R. Watson, "Drilling model for cutting lip and chisel edge and comparison of experimental and predicted results. II-reversed cutting lip model", *International Journal of Machine Tool Design and Research,* vol. 25, pp. 367-376 (1985).

[6] A.R. Watson, "Drilling model for cutting lip and chisel edge and comparison of experimental and predicted results. III-drilling model for chisel edge", *International Journal of Machine Tool Design and Research,* vol. 25, pp. 377-392 (1985).

[7] A.R. Watson, "Drilling model for cutting lip and chisel edge and comparison of experimental and predicted results. IV-drilling tests to determine chisel edge contribution to torque and thrust", *International Journal of Machine Tool Design and Research,* vol. 25, pp. 393-404 (1985).

[8] J.S. Agapiou and M.F. DeVries, "On the determination of thermal phenomena during a drilling process-part I, analytical models of twist drill temperature distributions", *International Journal of Machine Tools and Manufacture,* vol. 30, pp. 203-215 (1990).

[9] J.S. Agapiou and M.F. DeVries, "On the determination of thermal phenomena during a drilling process-part II, comparison of experimental and analytical twist

drill temperature distributions", *International Journal of Machine Tools and Manufacture,* vol. 30, pp. 217-226 (1990).

[10] D.A. Stephenson and J.S. Agapiou, "Calculation of main cutting edge forces and torques for drills with arbitrary point geometries", *International Journal of Machine Tools and Manufacture,* vol. 32, pp. 521-538 (1992).

[11] C. Rubenstein, "The torque and thrust force in twist drilling-II. comparison of experimental observations with deductions from theory", *International Journal of Machine Tools and Manufacture,* vol. 31, pp. 491-504 (1991).

[12] V. Chandrasekharan, S.G. Kapoor and R.E. DeVor, "A mechanistic approach to predicting the cutting forces in drilling: with application to fiber-reinforced composite materials", *Journal of Manufacturing Science and Engineering,* vol. 117, pp. 559-570 (1995).

[13] V. Chandrasekharan, S.G. Kapoor and R.E. DeVor, "A mechanistic model to predict the cutting force system for arbitrary drill point geometry", *Journal of Manufacturing Science and Engineering,* vol. 120, pp. 563-570 (1998).

[14] S. Min, D.A. Dornfeld, J. Kim and B. Shyu, "Finite element modeling of burr formation in metal cutting", *Machining Science and Technology,* vol.5, pp. 307-322 (2001).

[15] M. Shatla and T. Altan, "Analytical modeling of drilling and ball end Milling", *Journal of Materials Processing Technology,* vol. 98, pp. 125-133 (2000).

[16] M. Bono and J. Ni, "The effects of thermal distortions on the diameter and cylindricity of dry drilled holes", *International Journal of Machine Tools and Manufacture,* vol. 41, pp. 2261-2270 (2001).

[17] M. Bono and J. Ni, "A model for predicting the heat flow into the workpiece in dry drilling", *Journal of Manufacturing Science and Engineering,* vol. 124, pp. 773-777 (2002).

[18] J.S. Strenkowski, A.J. Shih and J.C. Lin, "An analytical finite element model for predicting three-dimensional tool forces and chip flow", *International Journal of Machine Tools and Manufacture,* vol. 42, pp. 723-731 (2002).

[19] J.T. Carroll and J.S. Strenkowski, “Finite element models of orthogonal cutting with applications to single point diamond turning”, *International Journal of Mechanical Science,* vol. 30, pp. 899-920 (1988).

[20] J.S. Strenkowski and K.J. Moon, “Finite element prediction of chip geometry and tool/workpiece temperature distributions in orthogonal cutting”, *Journal of Engineering for Industry,* vol. 112, pp. 313-318 (1990).

[21] S. Athavale and J.S. Strenkowski, “Material damage-based model for predicting chip-breakability”, *Journal of Manufacturing Science and Engineering,* vol. 119, pp. 675-680 (1997).

[22] A.J. Shih, “Finite element analysis of the rake angle effects in orthogonal metal cutting”, *International Journal of Mechanical Science,* vol. 38, pp. 1-17 (1996).

[23] M. Bono and J. Ni, “A method for measuring the temperature distribution along the cutting edges of a drill”, *Journal of Manufacturing Science and Engineering,* vol.124, pp. 921-923 (2002).

[24] J.S. Strenkowski, C.C. Hsieh and A.J. Shih, “An analytical finite element technique for predicting thrust force and torque in drilling**”,** *International Journal of Machine Tools & Manufacture,* vol. 44, pp. 1413-1421 (2004).

BIBLIOGRAPHY

[1] M. C. Shaw, “Metal cutting principles”, Third edition, M.I.T., Cambridge, Mass., 1954.

[2] V. Arshinov and G. Alekseev, “Metal cutting theory and cutting tool design”, Mir Publishers, Moscow, 1979.

[3] R. Tirupathi Chandrupatla and D. Ashok Belegundu, “Introduction to finite elements in engineering”, Prentice Hall of India Pvt. Ltd., New Delhi, 1997.

[4] O. C. Zienkiewicz, “The finite element method”, Tata McGraw-Hill Publication, London, 2003.

[5] J. N. Reddy, “Introduction to finite element method”, McGraw-Hill International Editions, London, 1993.

[6] David V. Hutton, “Fundamental of finite element analysis”, McGraw-Hill International Editions, London, 1994.

[7] R. Tirupathi Chandrupatla, “Finite element analysis for engineering and technology”, Universities Press, New Delhi, 2004.